

Mathematical Modeling of Snow Avalanches Movement

Samvel S. Grigorian, Alexander V. Ostroumov, Lomonossov State University, Institute of Mechanics, Moscow, Russia.

The problem of mathematical modeling of snow avalanche movement is basic for estimations and predictions of possible hazard parameters for given climatic and geographical conditions. There are three main problems in the general problem of quantitative description of snow avalanche phenomenon:

- 1) the problem of physics and mechanics of snow cover on the mountain slope and its evolution in time terminating by snow avalanche generation;*
- 2) the problem of snow masses motion over mountain slope;*
- 3) the problem of moving snow impact on obstacles and structures.*

The mathematical modeling of these processes requires application of different approaches and methods based on suitable schematizations of these complicated phenomena. A comprehensive survey of essential progress in this field with the analysis of the essence of necessary future investigations has been done years ago in Grigorian, 1974. Since that time many new results and publications appeared, but needs in more efficient and practically applicable efforts in this field yet are actual.

The subject of this work concerns with the analysis of modern state of this problem and with the presentation of several mathematical models for evaluation of main parameters of snow avalanche motion at different degree of simplification in mathematical and physical schematizations. Such a ranging of models is necessary and useful due to the needs in an instrument for quick, but sometimes rough estimations, in conditions where we have not necessary massive (a set) of initial information about the subject of investigation (the slope and the snow cover parameters etc.), in one case, and for more detailed quantitative description in a case when such a full information is available. In any case, in the course of the mathematical model constructing we do significant simplifications in mathematical characterization of moving snow masses introducing some averaged parameters and effective

values of physical-mechanical constants for flowing snow and for underlying bed. Of course, the adequacy of predictions by such a modeling should be established by comparison of obtained results with the observed data collected in natural conditions for given real geographical situation with possible subsequent corrections of model supporting by such data.

The problems of snow cover evolution and of snow flow impact are not touched here.

In the next parts of this work, the results of mathematical modeling of snow avalanches which has been done in the Department of Mechanics of Natural Processes at the Institute of Mechanics of the Moscow State University are presented and discussed. The work was fulfilled in the frame of contract with the Swiss Federal Institute for Snow and Avalanche Research, Davos.

Keywords: snow avalanche, mathematical model, snow capturing process, friction law, runout distance

Die Aufgabe der mathematischen Modellierung fuer die Bewegung der Schneelawinen dient als Grundlage fuer die Bewertung und Weissagung der moeglichen Parameterwerte von der Lawinengefahr fuer gegebene klimatischen und geographischen Verhaeltnisse. Man unterscheidet drei Hauptaufgabn im Gesamtproblem der quantitativen Beschreibung des Lawinenschneesturzes:

1) die Aufgabe der Physik und Mechanik fuer die Schneedecke auf den Berghaengen und ihre Evolution in der Zeit, die mit der Entstehung der Schneelavine beendet wird;

2) die Aufgabe ueber die Bewegung der Schneemasse durch die Berghang;

3) die Aufgabe ueber den Schlag des bewegenden Schnees an den Stoerungen und Anlagen.

Die mathematische Modellierung dieser Prozesse fordert die Anwendung von verschiedenen Herangehen und Methoden, die auf der passenden Schematisierung dieser komplizierten Erscheinungen gegrundet werden. Der ausfuehrliche Bericht des bedeutenden Progresses auf diesem Gebiet wurde mit der Analyse des Wesens der notwendigen zukuenftigen Forschungen vor viele Jahren in der Arbeit von Grigorian, 1974 ausgefuehrt. Seitdem wurde eine Menge von den neuen Ergebnissen und Veroeffentlichungen erschiehen,

aber das Beduerfnis nach den effektiven und praktisch verwendeten Ergebnissen wird auf diesem Gebiet wie vorher erhalten.

Als Gegenstand der vorliegenden Arbeit dient diese Analyse des modernen Zustandes dieses Problems und die Vorstellung von einigen mathematischen Modellen fuer die Bewertung der Hauptparameter von der Schneelawinenbewegung mit verschiedener Stufe der Vereinfachung in der mathematischen und physischen Schematisierung. Solche Verschiedenartigkeit der Modelle ist notwendig und vorteilhaft fuer den Bedarf an dem Instrument fuer schnelle, aber manchmal grobe Bewertungen im Falle, wenn wir einerseits keine notwendige Anfangsinformation ueber den Forschungsobjekt (Parameter des Berghanges und der Schneedecke usw) haben und andererseits, wenn solche volle Information fuer die detaillierte quatitative Beschreibung zur Verfuegung gestellt wird. Auf jeden Fall, im Laufe der Ausarbeitung der mathematischen Modelle machen wir bedeutende Vereinfachungen in der mathematischen Beschreibung der bewegenden Schneemassen und fuehren einige Durchschnittsparameter und effektive Werte der physisch-mechanischen Konstante fuer den laufenden Schnee und die Unterbettungsflaeche ein. Selbstverstaendlich muss die Aehnlichkeit der Weissagungen solcher Modellierung durch die Vergleichen der erhaltenen Ergebnisse mit den Beobachtungsdaten bewertet werden, die unter den Naturbedingungen fuer diese reale geographische Situation mit den moeglichen folgenden Vervollkommnungen der Modelle von gezeigten Daten gesammelt werden.

Die Entwicklungsprobleme der Schneedecke und des Schlages der Schneelawine wird hier nicht beruehrt.

In den nachfolgenden Teilen dieser Arbeit werden die Ergebnisse der mathematischen Modellierung fuer die Schneelawinen vorgestellt, die in der Abteilung fuer Mechanik der Naturprozesse des Institutes fuer Mechanik bei der Moskauerer Staatsuniversitaet erhalten wurden. Die Arbeit wurde in Rahmen des Kontraktes mit dem Schweizerischen Bundesinstitut fuer die Schnee- und Schneelawinenforschungen in Davos ausgefuehrt.

Keywords: Schneelawine, mathematische Modelle, Prozess der Schneeergreifung, Reibungsgesetz, Distanz des Auswurfes.

1. The full model

The problem of quantitative mathematical modeling of initiation and movement of snow masses on a mountain slope is rather complicated and bad posed due to the uncertainties in character of breaking and gradual fragmenting of snow in the course of starting and developing of snow fall process, and corresponding uncertainties in possibility of deriving of relations governing the mechanical interactions between the snow fragments and particles and the underlying soil or rock bed. In the first approximation, which is ordinarily sufficient for practical needs, we can consider a rough model introducing an averaging procedure — averaging the main characteristics of snow flow over space coordinate along the path of avalanche with a scale of averaging much more than the geometrical characteristics of the bed roughnesses and averaging over full local cross-section of the flowing snow mass.

Such a procedure leads to a so-called hydraulic model widely used in engineering hydraulics and giving sufficiently adequate results for practical purposes. So it is reasonable to hope that the hydraulic approach is also efficient in the case of mathematical modeling of snow avalanche dynamics.

According to above mentioned scheme, we shall use the following "full" mathematical model [Grigorian, Ostroumov, 1977]. The differential equations

$$\frac{\partial u}{\partial t} + u \frac{\partial u}{\partial S} = g \cdot \sin \psi - \frac{k \cdot u^2}{R} \operatorname{sign}(u) - \frac{L}{2F} \cdot \frac{\partial}{\partial S} \left(\frac{a \cdot F^2}{L^2} \right) - f_1 - f_2 \quad (1.1)$$

$$\frac{\partial F}{\partial t} + \frac{\partial(uF)}{\partial S} = q \quad , \quad (1.2)$$

$$\operatorname{sign}(u) = \begin{cases} 1, & u > 0 \\ 0, & u = 0 \\ -1, & u < 0 \end{cases} \quad , \quad a = g \cdot \cos \psi + \frac{u^2}{r}$$

Deriving the system of equations (1.1), (1.2) we have accepted a geometry of the surface underlying the moving snow masses as a channel with rectangular local cross-section varying with the longitudinal coordinate along the channel axis (the same structure of (1.1) we have also in the case when the geometry of channel cross-section is different but prescribed as a function of longitudinal coordinate). Here t , S are the time and space coordinate along avalanche route on the bed (see Fig. 1.1); $u(S,t)$, $F(S,t)$ are unknown values of S -component of snow velocity averaged over full cross-section of flow and the area of this cross-section; $L(S)$,

$\psi(S)$ are the local width of the cross-section and local inclination of the channel axis to the horizon; g is the gravity acceleration, $a(S,u)$ is the projection of the full acceleration (gravitational plus centrifugal) of the snow "particle" (remember the averaging u over cross-section and along S -coordinate with averaging scale much more than the depth of the flow) on the normal to the bed surface direction; k is hydraulic resistance coefficient; $R = FL/(L^2 + 2F)$ is so called hydraulic radius, r — curvature radius of channel axis. The values of f_1 , f_2 , q are specified as follows. According to [Grigorian, 1979; Grigorian, Ostroumov 1975], for the friction force f_1 on the bed surface we have an expression

$$f_1 = \begin{cases} \mu a \left(1 + \frac{h}{L}\right), & \text{if } \tau_1 = \mu \rho a h < \tau_* \\ \frac{\tau_*}{\rho h} \left(1 + \frac{2h}{L} - \frac{\tau_*}{L \mu \rho a}\right), & \text{if } \tau_1 \geq \tau_* \end{cases} \quad (1.3)$$

where μ is the Colomb friction law coefficient, ρ is the density of flowing snow, h is the local flow depth, τ_* is the upper limit of friction force appearing in modification of friction law of Grigorian, 1979 expressed as

$$\tau = \begin{cases} \mu p_n, & \text{if } \mu p_n \leq \tau_* \\ \tau_*, & \text{if } \mu p_n > \tau_* \end{cases} \quad (1.3a)$$

where p_n is the normal pressure on sliding surface.

The values f_2 , q relate to the process of capturing on the frontal surface of moving snow mass of the "fresh" snow being at rest on the slope. This process is difficult to model mathematically and our approach is as follows. We suppose that intensity of snow capturing representing by parameter q depends on the load p generating by moving snow on "fresh" snow. The scheme of the capturing process is shown on the Fig. 1.2. where h_0 is the thickness of the "fresh" snow, δ — the thickness in the zone where that snow is gradually involving in motion, ω is the velocity of propagation of the front of "fresh" snow breaking and coming in moving snow mass. Using the momentum and mass conservation laws we can write

$$\begin{aligned} \omega \rho_0 &= (\omega - v) \rho_1 \\ \omega v \rho_0 &= \begin{cases} p - p_*, & \text{if } p > p_* \\ 0, & \text{if } p \leq p_* \end{cases} \end{aligned} \quad (1.4)$$

where ρ_0 , ρ_1 are the densities of "fresh" and broken snow; ω , v are normal velocities of breaking front propagation and broken snow particles, p_* is the strength to breaking parameter, p is the full pressure (hydrostatic plus dynamic) on the bed ("fresh" snow) surface.

Relations (1.4) lead to

$$\omega = \sqrt{\frac{p - p_*}{\rho_0(1 - \rho_0/\rho_1)}} \equiv \sigma \cdot \sqrt{\frac{p - p_*}{\rho_0}}, \sigma \cong \text{const} \quad (1.5)$$

with parameter σ characterizing the compacting of the snow during breaking process. The pressure p is represented by relation

$$p = \rho(ah + Cu^2 \cdot \sin \alpha), \quad \alpha = \arctg\left(\frac{\partial \delta}{\partial S}\right) \quad (1.6)$$

where h and $\delta(S,t)$ are the local depth of moving snow and the local thickness of breaking snow cover, C is an empirical constant. Using (1.5) we get for mass source parameter q an expression

$$q = \omega \frac{\rho_0}{\rho \cdot \cos \alpha} L = \begin{cases} \frac{\sigma L}{\rho \cdot \cos \alpha} \sqrt{(p - p_*)\rho_0}, & p > p_* \\ 0, & p \leq p_* \end{cases} \quad (1.7)$$

where average density ρ is proposed to be generally different from ρ_1 . Above considerations lead also to the expression for force parameter f_2 as follows

$$f_2 = \begin{cases} \frac{qu}{F} + a \cdot \frac{\partial \delta}{\partial S}, & \text{if } \delta > 0 \\ 0, & \text{if } \delta = 0 \end{cases} \quad (1.8)$$

where condition $\delta = 0$ means that "fresh" snow sheet is completely destroyed and involved in motion at certain location behind the avalanche front.

Another expression for q can be derived by alternative consideration connecting the intensity of "fresh" snow cover erosion with shear forces giving the empirical relation of type

$$q = \xi [\rho(u^2 - u_*^2)]^n, \quad \xi, n, u_* - \text{const} \quad (1.7a)$$

but here we'll not discuss in details this alternative, which, of course, can be easily "implanted" in mathematical model.

Finally we have the set of relations (1.1), (1.2), (1.3), (1.6), (1.7), (1.8), giving the closed mathematical formulation of the model. For completion of this formulation for certain problem, which is to be solved in figures, it remains to formulate the initial and boundary conditions for the model.

The initial conditions are

$$u(S,0) = u_0(S), \quad F(S,0) = F_0(S) \quad (1.9)$$

where the functions $u_0(S)$, $F_0(S)$ are to be specified for concrete case under consideration.

The boundary conditions relate to the frontal and the "tail" parts of the snow flow. Regardless to the "fact" that the moving snow mass has not only a frontal sharp boundary moving along the slope but also the rear front also moving down the mountain surface, we suppose that this last front is not so sharp and important for the dynamics of main snow mass and accept more simple scheme of being at rest the rear "front" of avalanche. In other words, we will use the "tail" boundary conditions as follows

$$u(S_0, 0) = 0, \quad F(S_0, 0) = 0 \quad (1.10)$$

where S_0 is the coordinate (unchanged) of the back "front" of the avalanche.

The boundary conditions at the avalanche front are evident:

$$u(S_f, t) = w, \quad w = \frac{dS_f(t)}{dt}, \quad F(S_f, t) = 0 \quad (1.11)$$

where $S_f(t)$ is the coordinate of the front — a function of t to be determined in the course of the problem solution.

By this we complete the full mathematical formulation of the full initial-boundary value problem for snow avalanche dynamics mathematical modeling.

Now we start to consider a special case of the problem corresponding to the infinitely wide channel ($L \Rightarrow \infty$) giving a two-dimensional picture of motion, and for a situation when the slope is free of "fresh" snow. Such a simplification of the problem allows to get results in clear and easy for analysis and parametric comparisons form and gives a means for orientation in more complicated cases.

In such a specified case we have the differential equations

$$\frac{\partial u}{\partial t} + u \frac{\partial u}{\partial S} = g \cdot \sin \psi - f \cdot \text{sign}(u) - \frac{k \cdot u^2}{R} \text{sign}(u) - \frac{1}{2h} \cdot \frac{\partial}{\partial S} (ah^2) \quad (1.12)$$

$$\frac{\partial h}{\partial t} + \frac{\partial(uh)}{\partial S} = 0 \quad (1.13)$$

the initial conditions

$$u(S, 0) = u_0(S), \quad h(S, 0) = h_0(S), \quad (S \in [S_0, S_f(0)]) \quad (1.14)$$

and the boundary conditions

$$u(S_0, t) = 0, \quad h(S_0, t) = 0, \quad (1.15)$$

$$u(S_f(t), t) = w(t), \quad h(S_f(t), t) = 0. \quad (1.16)$$

Here t, S again are the time and the space coordinate along the avalanche route on the bed (see Fig.1.3), $S_f(t)$ is the coordinate of the avalanche front and so on; $h(S, t)$ is the local depth of

the avalanche; $u_0(S)$, $h_0(S)$ are initial distributions of $u(S,t)$ and $h(S,t)$ respectively; f is the friction force parameter determined by the relation

$$f = \begin{cases} \mu a, & \text{if } \tau_1 = \mu \rho a h < \tau_* \\ \frac{\tau_*}{\rho h}, & \text{if } \tau_1 \geq \tau_* \end{cases} \quad (1.17)$$

where again μ is the Colomb's friction coefficient, ρ is the density of flowing snow, τ_* is the upper limit for friction stress τ on the bed surface appeared in the modified friction law proposed in *Grigorian, 1979*. In the mathematical formulation of the problem (1.12)-(1.17), the set of values $\psi(S)$, $u_0(S)$, $h_0(S)$, μ , k , ρ , τ_* , is proposed known. The function $\psi(S)$ describes the geometry of the slope and, in principle, is known if the topography of the slope is available. The other values in this set are to be specified by the reasonable estimations of the mechanical properties of snow mass, depending on climatic and geographical factors and, for $u_0(S)$ and $h_0(S)$ — on the probable and "possible" initial distributions of u and h values.

The problem formulated in terms of full model allows to get the solution, generally speaking, only by numerical methods using the computer modeling. This is recommended for "precise" calculations when detailed information about necessary data ($\psi(S)$, k , etc.) is available and mathematical predictions are to be calculated as "exact" as possible. The formulation (1.12)-(1.17) gives necessary tool for such a work.

However in many real cases there are no definite information related to $\psi(S)$, μ and other necessary data. On the other hand, one often needs a more simple mathematical instrument for estimations by an explicit formula or by simple computations without "heavy" computer modeling. For such purposes, we can construct different kind of simplified models which derivation is the content of the following parts of this work.

2. The simplified version of the full model

The possible procedure of simplification considered initially in *Grigorian, Ostroumov, Stacheiko, 1979* is as follows. In the right hand side of (1.1) we neglect the two last terms and rewrite the resulting equation in Lagrangian coordinate system to have

$$S = S(\xi, t), \quad u = \frac{\partial S}{\partial t}, \quad (2.1)$$

where ξ is Lagrangian coordinate. As a result instead of (1.1) one has

$$\frac{1}{2} \frac{\partial u^2}{\partial S} = g \cdot \sin \psi - f \cdot \text{sign}(u) \quad (2.2)$$

The second step of the simplification procedure consists of introduction of integrated form of the mass conservation law instead of differential form (1.13). An integration of $h(S,t)$ over coordinate S leads to the relation

$$F(t) = \int_{S_0}^{S_f(t)} h(S,t) dS = \kappa H l = \text{const} = F_0 \quad (2.3)$$

where $F_0 = F(0)$, $H = \max_S(h(S,t))$, $l = S_f(t) - S_0$ and κ is a parameter characterizing the "fullness" of the graph of $h(S,t)$. Now we accept an important and "responsible" hypotheses of constancy of the κ parameter. Of course, κ changes in time, but as it will be demonstrated by comparison of numerical results obtained on the basis of the full and simplified models, the deviations of κ from a constant value are not dramatic and therefore this hypothesis looks acceptable for estimations.

To evaluate the model (2.1)-(2.3) by simple calculating means one can divide the avalanche path on several intervals introducing dividing points $S_0, S_1, S_2, \dots, S_N$ with negligible change in $\psi(S)$ within an interval $S_i \leq S \leq S_{i+1}$. This allows to integrate (2.2) over $[S_i, S_{i+1}]$ and to get the relation

$$u^2(S) = u^2(S_i) + 2(S - S_i) [\overline{g(\sin \psi)}_i - \overline{f}_i] \quad (2.4)$$

where

$$\overline{(\sin \psi)}_i = \frac{1}{S_{i+1} - S_i} \int_{S_i}^{S_{i+1}} \sin \psi dS, \quad \overline{f}_i = \frac{1}{S_{i+1} - S_i} \int_{S_i}^{S_{i+1}} f dS \quad (2.5)$$

(we consider only the case $u > 0$, $\text{sign}(u) = 1$). To calculate velocity u by (2.4), we need an information about h to calculate \overline{f}_i by (2.5). As it is demonstrated by the results of full model calculations, the main important unknown parameters of avalanche — velocity, depth and runout distance are mainly determined by the parameters in the flow zone near the coordinate with the maximal value of h . The full model calculations show that this region is closely attached to the avalanche front and the Lagrangian coordinate of the phase with $h = \max(h)$ is slightly changing with time. By this reason we can suppose for further simplification of calculations that this coordinate remains unchanged in time and coincides

with the Lagrangian coordinate of the avalanche front. All this considerations allow us to use the value $H = \max(h)$ instead of h when calculating $\overline{(f)}_i$, and calculate l by the relation

$$l = S - S_0 \quad (2.6)$$

substituting S instead of S_f because S -coordinates in the significant for all dynamics zone near the cross-section with $H \cong \max(h)$ are close to S_f . In *Grigorian, Ostroumov, Stacheiko, 1979* the value $\kappa \cong 0.3 \div 0.4$ is recommended for parameter κ in the case when geometry of slope is changed smoothly with S .

Of course to have an impression relating to the accuracy and approximating ability of simplified model presented here one needs to make parallel calculations for the same problem using full and simplified models and compare the results. Such a work has been done and the results obtained are presented in the next part.

3. Comparison of the computations by the full and simplified models

The calculations for the full model were performed for simple geometry with $\psi = \text{const}$. At the initial interval of the slope $S_0 = 0$, $S_f(0) = 100$ m different distributions $h_0(S)$, $u_0(S)$ were prescribed, as well as different combinations of the values of parameters μ , k , ρ , τ_* , ψ also were tested. The basic variant was with $\psi = 30^\circ$, $\mu = 0.5$, $k = 0.02$, $\rho = 50 \text{ kg}\cdot\text{s}^2/\text{m}^4$, $\tau_* = 1000 \text{ kg}/\text{m}^2$. The $h_0(S)$ was taken in triangular and parabolic forms with variable value of H_0 ; for $u_0(0)$ a uniform distribution was used (see Fig. 3.1). On the Fig. 3.2a the calculated by full model distribution of h/H over S at subsequent instants of motion are presented. On the Fig. 3.2b the distributions over S_f (corresponding to different time t) of κ , H , w , S^*/S_f , where S^* is the S -coordinate of the point where $h = \max(h) = H$, are presented. All these data relate to the basic variant. Fig. 3.3-3.11 illustrate analogous results for other variants calculated.

Tab. 3.1: The set of numerical values of the problem parameters for tested variants.

Variant N	μ	k	τ kg/m^2	ρ $\text{kg}\cdot\text{s}^2$	ψ grad	U_0 m/s	H_0 m	Profile $h_0(s)$
--------------	-------	-----	----------------------------------	--------------------------------------	----------------	--------------	------------	------------------

				m ⁴				
1	0.5	0.02	1000	50	30	10	1	parabola
2	0.5	0.02	1000	50	30	1	10	parabola
3	0.5	0.02	1000	50	30	10	10	triangle
4	0.5	0.02	1000	50	30	10	1	triangle
5	0.5	0.02	1000	50	30	10	1	parabola
6	0.5	0.02	1000	50	30	10	60	triangle
7	0.5	0.02	1000	50	46	1	10	parabola
8	0.25	0.02	1000	50	30	1	10	parabola
9	0.5	0.06	1000	50	30	1	10	parabola
10	0.5	0.02	250	50	30	1	10	parabola

Tab 3.2: The results of calculations by full and simplified theories are presented in terms of w and H as functions of S_f .

($\kappa = 0.36$)

Variant N	S_f	w		H	
		full model	formula (2.4)	full model	formula (2.3)
1	100	1.00	1.00	1.000	
	200	5.23	11.49	0.722	0.929
	600	3.37	25.61	0.323	0.309
	1000	2.60	34.35	0.200	0.185
	1400	2.22	41.27	0.146	0.132
2	100	1.00	1.00	10.00	
	200	18.48	25.64	4.733	9.290
	400	13.50	36.39	2.900	3.620
	600	8.46	39.83	1.973	3.090
	1000	7.60	45.95	1.607	1.850
	1400	6.64	51.35	1.272	1.320
7	100	1.0	1.00	10.00	18.52
	200	28.0	32.00	6.25	9.29
	400	28.5	51.00	4.00	4.63
	600	25.5	64.00	3.00	3.09
	1000	21.2	84.14	2.20	1.85
	1400	16.0	100.0	1.50	1.32
	2000	14.0	120.0	1.00	0.93
2500	12.0	134.0	0.75	0.74	
	100	1.00	1.00	10.00	18.52
	200	21.5	25.64	4.8	9.29
	400	23.5	42.10	3.5	4.63

8	600	21.6	53.67	2.9	3.09
	1000	17.0	71.63	2.0	1.85
	1400	14.7	78.83	1.7	1.54
9	100	1.00	1.00	10.00	18.52
	200	13.5	25.64	4.90	9.29
	400	5.9	36.39	2.70	4.63
	600	5.3	39.83	2.25	3.09
	1000	4.8	45.95	1.65	1.85
	2000	4.2	48.70	1.50	1.54

The Table 3.1 indicates the correspondence between the variant's number and values of parameters. The general feature of the solution for all the variants consists in fast transformation of the solution into asymptotic form independent of initial distribution.

Asymptotic distribution of h approximately can be described by the relation $h/H = (S/S_f)^2$ and the values of H , w , S^*/S_f become smooth and slowly varying functions of t with $S^*/S_f \Rightarrow 1$, $\kappa \Rightarrow 0.36$ for all the variants calculated.

Note that asymptotic behavior of the solution appears after "spreading" of avalanche body with $H < h^* = \tau^*/(\rho a \mu)$, or, in other words, when Colomb friction law governs all the avalanche parts. Before this stage significant changes in κ , S^*/S_f are visible and character of these changes depends essentially on initial data.

As a conclusion we can mention that the flow asymptotical simplification with $\kappa = \text{const}$, $S^*/S_f = \text{const} \cong 1$ will appear in cases with slowly changing slope geometry and for this very case the simplified model is acceptable for simple estimations. In the table 3.2 the results of calculations by full and simplified theories are presented in terms of w and H as functions of S_f . One can see that the simplified theory gives acceptable accuracy for H and overestimates the

values of velocity w . This last effect is mainly due to the neglecting of resistance term $-ku^2/h$ in the momentum equation in simplified model and indicates on necessity of improvement of simplified theory. Such an improvement is presented in the next part.

4. Improvement of simplified model

Including in the momentum equation the inertial term $-ku^2/h$ and using all other simplifying considerations of previous part we get the relations

$$\frac{1}{2} \frac{\partial u^2}{\partial S} = g \cdot \sin \psi - f - \frac{ku^2}{H} \quad (4.1)$$

$$H = \frac{F_0}{\kappa l} \quad (4.2)$$

and introducing the definitions:

$$A = \begin{cases} 2(g \cdot \sin \psi - \mu a), & \text{if } \tau = \mu \rho a H < \tau_* \\ 2g \cdot \sin \psi, & \text{if } \tau \geq \tau_* \end{cases} \quad (4.3)$$

$$B = 2k\kappa / F_0, \quad (4.4)$$

$$D = \begin{cases} 0, & \text{if } \tau < \tau_* \\ 2\tau_* \kappa / (\rho F_0), & \text{if } \tau \geq \tau_* \end{cases} \quad (4.5)$$

we can rewrite (4.1) in the form

$$\frac{\partial u^2}{\partial S} = A - Bu^2S - DS \quad (4.6)$$

The solution of (4.6) on the intervals $S \in [S_i, S_{i+1}]$ with initial condition

$$u(S_i) = u_{0i} \quad (4.7)$$

is given by the relation

$$u(S) = \sqrt{-\frac{D}{B} + A \cdot \exp\left(\frac{BS^2}{2}\right) \cdot \int_{S_i}^S \exp\left(\frac{Bx^2}{2}\right) dx + \left(u_{0i}^2 + \frac{D}{B}\right) \exp\left(\frac{B}{2}(S_i^2 - S^2)\right)} \quad (4.8)$$

where in calculations of A, B, D one should use the average of ψ over the interval $[S_i, S_{i+1}]$.

Denoting by definition

$$Z(\xi) \equiv \exp(-\xi^2/2) \int_0^\xi \exp(x^2/2) dx \quad (4.9)$$

with $\xi = S\sqrt{B}$ we get

$$u(S) = \sqrt{-\frac{D}{B} + \frac{A}{\sqrt{B}} Z(\sqrt{B} S) + \left(u_{0i}^2 + \frac{D}{B} - \frac{A}{\sqrt{B}} Z(\sqrt{B} S_i)\right) \exp\left(\frac{B}{2}(S_i^2 - S^2)\right)} \quad (4.10)$$

The graph of $Z(\xi)$ is shown on Fig. 4.1.

Consider now the qualitative features of solutions of (4.6). Using a new variable y :

$$y = u^2 + D/B \quad (4.11)$$

we have instead of (4.6) the equation

$$y' = A - BSy \quad (4.12)$$

and as $u^2 = y - D/B \geq 0$ we will be interested only in solutions of (4.12) satisfying the conditions $y \geq D/B \geq 0$.

On the y, S plane the hyperbolas $yS = \gamma = \text{const}$ are the isoclines of (4.12) where $y' = \text{const}$. On the hyperbolas $\gamma S = A/B$ we have $y' = 0$ so all the solutions have there extremes (maxima, for if $\gamma < A/B$ then $y' > 0$ and at $\gamma > A/B$ $y' < 0$). As a result we can imagine a picture of equation (4.12) integral curves distribution, shown on Fig. 4.2. Depending on initial data an integral curve tends (when $S \rightarrow \infty$) to hyperbola

$$y = A/BS \quad (4.13)$$

monotonically or after some initial rise to maximum of y with subsequent tending to (4.13) as $S \rightarrow \infty$. It can be easily shown that at the curve

$$y = \frac{AS}{BS^2 - 1} \quad (4.14)$$

we have $y'' = 0$ and at any given point of (4.14) with coordinate $S = S_*$ a solution of (4.12) touches some hyperbola $yS = \gamma_*$ depending on initial data and for $S > S_*$ the solution becomes "captured" between the curve (4.14) and hyperbola $yS = \gamma_*$. This leads to simple estimations for large values of S as follows

$$\frac{A}{BS} < \frac{AS}{BS^2 - 1} < y < \frac{\gamma_*}{S} \quad (4.15)$$

On the basis of this improved model a series of calculations have been performed with the same numerical examples as for non-improved model and the results are shown in Table 4.1, illustrating the work (the performance) of improved model when compared with "exact" results of the full model. One can conclude that correspondence between these sets of results is very good in a wide range of main parameters of the problem. At large values of S , even simplest relation (4.13) delivers high accuracy of estimations. Note that all these calculations were performed for value of $\kappa = 0.36$. So this figure can be recommended for practical needs over wide range of parameters.

Tab. 4.1 ($\kappa = 0.36$)

Variant N	S_f	w			
		full model	formula (4.10)	full (4.14)	formula (4.13)
1	100	1.00	1.00	(10.64)	(7.8)
	200	5.23	5.98	5.862	5.51
	600	3.37	3.21	3.203	3.18
	1000	2.60	2.60	2.469	2.47
	1400	2.22	2.09	2.080	2.08
2	100	1.00	1.00	-	(24.65)
	200	18.48	23.45	-	17.43
	400	13.50	21.13	14.62	12.32
	600	8.46	10.96	10.78	10.07
	1000	7.60	8.01	7.78	7.80
	1400	6.64	6.68	6.67	6.59
7	100	1.0	1.00	-	(58.17)
	200	28.0	30.12	-	41.13
	400	28.5	30.52	34.49	29.10
	600	25.5	25.82	25.45	23.75
	1000	21.2	18.88	18.84	18.38
	1400	16.0	15.74	15.73	15.52
	2500	14.0	13.09	13.08	13.01
	2500	12.0	11.75	11.68	11.63
8	100	1.00	1.00	-	(50.72)
	200	21.5	21.60	-	35.86
	400	23.5	26.60	30.07	25.36
	600	21.6	22.51	22.18	20.69
	1000	17.0	16.47	16.42	16.03
	1400	14.7	14.89	14.88	14.63
9	100	1.00	1.00	-	(14.23)
	200	13.5	18.41	12.84	10.06
	400	5.9	7.92	7.49	7.11
	600	5.3	5.95	5.94	5.81
	1000	4.8	4.54	4.54	4.50
	2000	4.2	4.14	4.14	4.11

5. The simplest model for rough estimations

In the literature one can find many articles where very simple scheme for snow avalanche dynamics is used. In this scheme, the avalanche is considered as a material point neglecting

spatial dimensions of flowing snow mass and changes in time of these dimensions. Here we will consider the problem in this case and establish what kind of hypotheses we should accept to derive such a model from "exact" one. The main differential equations of material point model are as follows

$$\frac{dS}{dt} = u, \quad m \frac{du}{dt} = mg \cdot \sin \psi - r \quad (5.1)$$

where m is the "point's" mass proposed to be constant, r is resistance force — force of interaction between moving body and underlying base surface, other denotations are as before. We can write a relation

$$m = \rho H l b \quad (5.2)$$

where ρ is the snow density, supposed (assumed) constant, H , l , b are the height, length and width of the avalanche body respectively. For the resistance r we have

$$r = l b \tau \quad (5.3)$$

where τ is average specific frictional stress on the bed surface. So we reduce (5.1)-(5.3) to

$$\frac{dS}{dt} = u, \quad \frac{du}{dt} = g \cdot \sin \psi - \tau / \rho H \quad (5.4)$$

and it is obvious that to derive equation (5.4) from corresponding momentum equation of the full model (1.1) we must neglect the term representing the gradient of normal force acting at the cross-section of the avalanche body, the term $(\rho g / 2F) \cdot \partial F / \partial S$, and include (or not) the hydrodynamic resistance term — the term $-k \rho u^2 / R$, in an expression for τ . Till now there is no difference between simplified model of part 2 and that under consideration here. Such a difference appears when we look at the next simplification in this simplest "point-mass" model supposing constancy of the parameter H . As it is visible from the results of calculations by the full or simplified models, the parameter H varies significantly in the course of the avalanche propagation along the mountain slope. Nevertheless one can hope that for rough estimations, it is possible to apply the simplest "effective" value for $H = \text{const}$.

Consider now the evaluation of simplest model for several hypothesis about resistance force τ .

5.1. Often in the point-mass model calculations the Colomb friction law is used leading to the expression for τ as follows

$$\tau = \mu p_n, \quad p_n = \rho g H \cdot \cos \psi \quad (5.5)$$

and the hydrodynamic (quadratic in u) term neglected. In this case, the problem allows the solution in quadratures

$$u^2 = u_0^2 + 2g \cdot \int_{S_0}^S [\sin \psi(\xi) - \mu \cdot \cos \psi(\xi)] d\xi, \quad (5.6)$$

$$u_0 t = \int_{S_0}^S \frac{d\xi}{\sqrt{1 + \frac{2g}{u_0^2} \int_{S_0}^{\xi} [\sin \psi(\xi) - \mu \cdot \cos \psi(\xi)] d\xi}} \quad (5.7)$$

where S_0 , u_0 are the initial position and velocity of the avalanche body.

For given geometry of slope the right hand sides of (5.6), (5.7) are known functions of S (as $\psi(S)$ is known). So the numerical evaluation of these expressions are reduced to rather simple calculations. Note that if the slope is steep enough, i.e. $\sin \psi - \mu \cdot \cos \psi > 0$, the avalanche motion will accelerate in time. In opposite case the motion decelerates and even stops on the slope if the length of the path on the inclined part of the trajectory is long enough.

To have explicit formula and be able to make clear analysis of the avalanche behavior in qualitative and quantitative manner, we suppose that the avalanche path consists of two parts: the first inclined to the horizon with $\psi = \text{const}$ and the second horizontal one. Using (5.6) we have

$$u = u_0 \cdot \sqrt{1 + 2g \cdot (\sin \psi(\xi) - \mu \cdot \cos \psi(\xi)) (S - S_0) / u_0^2} \quad (5.8)$$

and denoting $l_1 = S_1 - S_0$, where S_1 is the coordinate of the end of the first part of the slope, we get for initial velocity for the second part an expression

$$u_1 = u_0 \cdot \sqrt{1 + 2g \cdot (\sin \psi(\xi) - \mu \cdot \cos \psi(\xi)) \cdot l_1 / u_0^2} \quad (5.9)$$

Using (5.6) for that part with (5.9) instead of u_0 and substituting $\psi = 0$ we have

$$u = u_1 - 2g\mu \cdot (S - S_1) \quad (5.10)$$

At the second part of the path the motion is decelerating and at some distance S_2 it decays completely. So for this distance we have (putting $u = 0$, $S = S_2$ into (5.10))

$$l_2 = S_2 - S_1 = \frac{u_1^2}{2g\mu} \quad (5.11)$$

Note that this runout distance l_2 does not depend at all on avalanche size.

Using (5.9), (5.11) and the definition of l_1 we have for full runout distance $L = S_2 - S_0$ an expression

$$L = S_2 - S_0 = \frac{u_0^2}{2g\mu} + \left[1 + (\sin \psi / \mu - \cos \psi)\right] \cdot l_1 \quad (5.12)$$

If $(\sin \psi - \mu \cdot \cos \psi) < 0$ the avalanche stops on the slope, otherwise a definite runout distance on horizontal part will occur.

We can now easily take into account the influence of quadratic in velocity resistance term in this simplest model to have:

for initial part of the path

$$u = u_0 \cdot \sqrt{1 - \frac{gh \cdot (\sin \psi - \mu \cos \psi)}{k \cdot u_0^2} \cdot \left(\exp\left[-\frac{2k}{H}(S - S_0)\right] - 1\right)} \quad (5.13)$$

$$u_1 = u_0 \cdot \sqrt{1 - \frac{gh \cdot (\sin \psi - \mu \cos \psi)}{k \cdot u_0^2} \cdot \left(\exp\left[-2kl_1/H\right] - 1\right)} \quad (5.14)$$

instead of (5.8), (5.9);

for horizontal part of the path

$$u = u_1 \cdot \sqrt{1 - \frac{gh \cdot (\sin \psi - \mu \cos \psi)}{k \cdot u_0^2} \cdot \left(\exp\left[-\frac{2k}{H}(S - S_1)\right] - 1\right)} \quad (5.15)$$

so if we put $u = 0$ here we get for $l_2 = S_2 - S_1$

$$l_2 = S_2 - S_1 = \frac{H}{2k} \cdot \ln\left(1 - \frac{ku_0^2}{\mu gH} + \left[\exp(-2kl_1/H) - 1\right] \cdot \frac{(\sin \psi - \mu \cos \psi)}{\mu}\right)^{-1}$$

instead of (5.11).

Finally we have for full runout distance

$$L_2 = l_1 + \frac{H}{2k} \cdot \ln\left[1 - \frac{ku^2}{\mu gH} + \left[\exp(-2kl_1/H) - 1\right] \cdot \frac{(\sin \psi - \mu \cdot \cos \psi)}{\mu}\right]^{-1} \quad (5.16)$$

Of course when $k \rightarrow 0$ the (5.13)-(5.16) transforms into (5.8)-(5.12). Note again that in this case the runout distance does not depend on avalanche mass (or size), which feature is characteristic for the Colomb resistance law application to avalanche dynamics calculation. This case may be reasonable for situations with rather small avalanches (of small thicknesses).

5.2. Consider now the case of very big avalanches (with big snow depth H) when almost everywhere in the avalanche body the thickness H is large enough — bigger than $H_* = \tau_*/\mu\rho \cdot \cos\psi$ when the friction law $\tau = \tau_* = \text{const}$ is applicable instead of the Colomb law. In this case we have (after integrating (5.3)) the following relations for initial part of the avalanche path

$$u = u_0 + \left(g \cdot \sin \psi - \frac{\tau_*}{\rho H} \right) \cdot t, \quad S - S_0 = u_0 t + \frac{1}{2} \left(g \cdot \sin \psi - \frac{\tau_*}{\rho H} \right) \cdot t^2 \quad (5.17)$$

At the mountain foot, $S - S_0 = S_1 - S_0 = l_1$, we have $t = t_1$

$$u = u_1 = u_0 + \left(g \cdot \sin \psi - \frac{\tau_*}{\rho H} \right) \cdot t_1, \quad l_1 = u_0 t_1 + \frac{1}{2} \left(g \cdot \sin \psi - \frac{\tau_*}{\rho H} \right) \cdot t_1^2 \quad (5.18)$$

and

$$t_1 = \frac{\sqrt{u_0^2 + 2 \left(g \cdot \sin \psi - \frac{\tau_*}{\rho H} \right) \cdot l_1} - u_0}{g \cdot \sin \psi - \frac{\tau_*}{\rho H}} \quad (5.19)$$

$$u_1 = \sqrt{u_0^2 + 2 \left(g \cdot \sin \psi - \frac{\tau_*}{\rho H} \right) \cdot l_1}$$

For the second (horizontal) part we have

$$u = u_1 - \frac{\tau_*}{\rho H} \cdot t, \quad S - S_1 = u_1 t - \frac{\tau_*}{2\rho H} \cdot t^2 \quad (5.20)$$

and at $S - S_1 = S_2 - S_1 = l_2$ where $u = 0$ we have

$$t = t_2 = \frac{\rho H u_1}{\tau_*} = \frac{\rho H}{\tau_*} \cdot \sqrt{u_0^2 + 2 \left(g \cdot \sin \psi - \frac{\tau_*}{\rho H} \right) \cdot l_1} \quad (5.21)$$

$$l_2 = u_1 t_2 - \frac{\tau_*}{2\rho H} \cdot t_2^2 = \frac{\rho H}{2\tau_*} \cdot \left(u_0^2 + 2 g l_1 \sin \psi \right) - l_1 \quad (5.22)$$

The full distance $L = l_1 + l_2$ is given by the relation

$$L = \frac{\rho H}{2\tau_*} \cdot \left(u_0^2 + 2 g l_1 \sin \psi \right) - l_1 \quad (5.23)$$

Note now that important feature of obtained relations in this case is their significant dependence of the avalanche size H . Particularly interesting is the dependence of runout

distance L on H : the bigger (dipper) is the avalanche the longer is its runout. In this respect big avalanche governing by the limiting friction force law with $\tau = \tau_* = \text{const}$ differs significantly from a small avalanche governed by classic Colomb law.

This conclusion is, of course, valid not only for the simplest model considered here but also for exact ones representing the physical difference between the two friction laws examined. The restriction in shear forces acting on the avalanche bed by the limiting value τ_* leads to extremely high movability of the snow flow on the mountain slope and foot with dramatical rise of runout distances in the range of big avalanches.

It is interesting also to see how looks the result when taking into account the hydraulic resistance representing by the term $-ku^2/H$ in equation (5.3). In this case integration for initial part of the path gives

$$u^2 = u_*^2 + (u_0^2 - u_*^2) \cdot \exp\left[-\frac{2k}{H} \cdot (S - S_0)\right], \quad u_*^2 \equiv \frac{H}{k} \cdot \left(g \cdot \sin \psi - \frac{\tau_*}{\rho H}\right) \quad (5.24)$$

$$u_1^2 = u_*^2 + (u_0^2 - u_*^2) \cdot \exp\left[-\frac{2k}{H} \cdot l_1\right] \quad (5.25)$$

and for second part

$$u^2 = (u_{**}^2 + u_1^2) \cdot \exp\left[-\frac{2k}{H} \cdot (S - S_1)\right] - u_{**}^2, \quad u_{**}^2 = \frac{\tau_*}{\rho H k} \quad (5.26)$$

For the runout distance $S_2 - S_1 = l_2$ we have from (5.26) and $u(S_2) = 0$

$$l_2 = \frac{H}{2k} \cdot \ln\left(\frac{u_1^2}{u_{**}^2} + 1\right) = \frac{H}{2k} \cdot \ln\left(1 + \frac{\rho H}{\tau_*} \left[g \cdot \sin \psi - \frac{\tau_*}{\rho H}\right] + \frac{\rho k}{\tau_*} \cdot \left(u_0^2 - \frac{H}{k} \left[g \cdot \sin \psi - \frac{\tau_*}{\rho H}\right]\right) \cdot \exp\left[-\frac{2k}{H} \cdot l_1\right]\right) \quad (5.27)$$

Considering (5.27) with $k \rightarrow 0$ one can see that (5.27) naturally turns into (5.22).

The strong dependence of l_2 on avalanche size H given by (5.27) is obvious and all the conclusions relating to the properties of big avalanches made above in the most simple case with $k = 0$ remain unchanged. However the influence of hydraulic resistance term is also significant for linear relationships (5.22), (5.23) between runout distance and avalanche size H changes in more complicated one, (5.27), containing logarithmic and exponential functions. As a result runout l_2 rises with increase in H much more slowly than it is predicted by linear relations (5.22), (5.23).

Consider a numerical example corresponding to the following data: $k = 0.02$; $\tau_* = 1000$ kg/m²; $\rho = 50$ kg·s/m⁴; $\mu = 0.5$; $\sin\psi = 0.5$; $g = 10$ m/s²; $l_1 = 1000$ m; $H = 5$ m; $u_0 = 0$. Calculation by (5.12) (Colomb friction law) gives $l_2/l_1 = 0.125$, $l_2 = 125$ m. By the relation (5.22) in a case of limited friction force we have $l_2/l_1 = 0.25$, $l_2 = 250$ m. In this case, the lower value of $H = H_*$ restricting the range of avalanche depth for applicability of limited shear law is equal to $H_* = \tau_*/\mu\rho g = 4.57$ m. So the value $H = 5$ m used in the calculations is only slightly above H_* . Value of l_2 for this law is only twice higher than that in the case of Colomb law. More adequate seems the value of $\tau_* = 500$ kg/m², in which case we have $H_* = 2.3$ m and $l_2/l_1 = 1.5$ when $H = 5$ m. One can see that in this case runout l_2 is one order of magnitude more than that for Colomb law.

Consider now influence of hydraulic resistance on these figures. Using the relation (5.15) for the Colomb law we have

$$l_2/l_1 \approx -H \cdot \ln\left[1 - \left(\sin\psi/\mu - \cos\psi\right)\right]/2k l_1 \approx -\ln[1 - (1 - 0.785)]/8 \approx 0.125/8.$$

By the relation (5.27) we obtain

$$l_2/l_1 \approx -H \cdot \ln\left[1 + \rho g H (\sin\psi - \tau_*/\rho g H)/\tau_*\right]/2k l_1 \approx \ln[1 + 0.25]/8 \approx 0.25/8.$$

The last figures show that the influence of quadratic resistance is strong enough and reduces the runout distance significantly. But in this case the runout distance based on the Colomb law remains much less than that in the case of limited friction force law. Note also that in both cases the reduction of the runout distance by the quadratic resistance seems to be highly overestimated. In this respect the problem of adequate estimation of hydraulic part of resistance remains actual and needs additional researches.

6. Influence of snow capturing on avalanche dynamics

Now we return to numerical examination of full model to see how the "fresh" snow capturing at the front of propagating avalanche influences on avalanche dynamics. We have fulfilled a series of full model computations for simple situation with constant thickness of "fresh" snow cover on a plane slope and with varying parameters of problem (μ , k , etc.). The results are presented on figures 6.1 - 6.7 (on these figures the scale for abscissa for 10 m adjacent to the

front of avalanche is the same as for h , h_0 parameters, whereas for the rest part of S -axis the scale is highly stretched).

One can see that depending on specific combination of values of governing parameters of the problem the avalanche behavior can be related to two quite different types, one of which is characterized by intensive "fresh" snow capturing in frontal zone and huge avalanche "head" formation in that zone, and another one which is unable to maintain the "fresh" snow erosion even when in the starting zone such capturing had appeared, resulting the "weak" avalanche formation with flattening of the avalanche body and decaying the whole process. It is very important to note, that which alternative of this two will take place depends on values of governing parameters (μ , k , etc.) nonmonotonically. As an example, on the fig.6.5 we can see that in the range of μ values $0.4 \leq \mu \leq 0.55$ the avalanche dynamics corresponding to the side values relates to the second ("weak") type, but for middle value of $\mu = 0.42$ that is of the first type! Of course, the reason for such a "strange" dependence of mathematical solution of the avalanche dynamics problem is due to the strong nonlinearity of that. Physical nature of this nonmonotonic behavior is associated with features of modified friction law of *Grigorian*, 1979. Indeed, when everywhere the avalanche thickness is sufficiently small, so everywhere $\tau < \tau_*$, and there is no influences on the process leading to the accumulation of snow in the avalanche body resulting the appearance of condition $\tau > \tau_*$ there, the avalanche dynamics remains "weak" all time of the motion. If, in contrast, there is a reason for mentioned accumulation process (e.g. due to sharp changes in cross-section area of channel, local big values of "fresh" snow thickness etc.), the avalanche behavior changes in that zone in accordance with the friction law ($\tau > \tau_*$), avalanche becomes selfexciting ("self-supporting") and highly movable. As a result the "output" parameters of avalanche (characteristic velocities, thickness, runout distance etc.) become dependent on initial parameters stochastically and nonpredictable. This feature of avalanche dynamics is the most interesting in mathematical sense and very important for general understanding of avalanche problem.

7. Conclusions

The results of analytical and computational investigations presented here show that the mathematical problem of quantitative description of snow avalanche dynamics is highly

nonlinear and difficult for receiving (obtaining) a simple explicit solutions. On the other hand, there is the necessity to have such a simple explicit relations for practical estimations. Unfortunately this need cannot be satisfied in desired form for only rough estimations are possible on the basis of very "finite" simplifications made with more or less exact full models. Corresponding procedures are presented and illustrated by numerical calculations in this paper.

One of the most important parameters for practical applications is the maximal runout distance of avalanches at given geographical and climatic conditions. The maximal runout distance corresponds to the most powerful and massive avalanches in which case one can expect the details of "exact" full model to be not significant. The correct approximate result presumably can be obtained in this case by simplified model or even by simplest model described above.

More difficult is the problem of quantitative description of avalanche motion evolution and decay depending on uncertain information relating to natural data ($\psi(S)$, μ , ρ , τ_* etc.) and mathematical modeling of the process of recruitment of "fresh" snow in the avalanche body in the frontal zone. The computational simulation of the avalanche dynamics made on the basis of the full model show that avalanche behavior is in some sense stochastic. Namely, depending on slight differences in initial data, bed geometry etc., mass velocities, depth distribution and other parameters of motion demonstrate finite differences and pulsatile behavior in the course of avalanche propagation over the mountain slope. This phenomenon is associated with dual nature of bed resistance law: the transitions between the Colomb's law and the τ_* -law appears with the changes in depth distribution $H(S)$ which itself is dependent nonlinearly on the resistance law. This stochasticity of avalanche dynamics makes the full problem not describable in deterministic way and only statistic characteristics of the main avalanche parameters calculated by the full model which itself is deterministic are to be evaluated and used for practical needs.

Nevertheless there is a program for improvement of "exact" full model consisting in testing of various schemes of snow capturing at the avalanche front and in more adequate modelling of hydraulic or viscous part of resistance as well as in making complete software involving all the components of mathematical construction and parameter variations in the problem. This work remains yet to be done.

References

GRIGORIAN, S.S., 1974: Mechanics of snow avalanches. In: Snow Mechanics - Symposium - *Mechanique de la Neige*. (Proceedings of the Grindelwald Symposium, April, IAHS - AISH Publ., N 114).

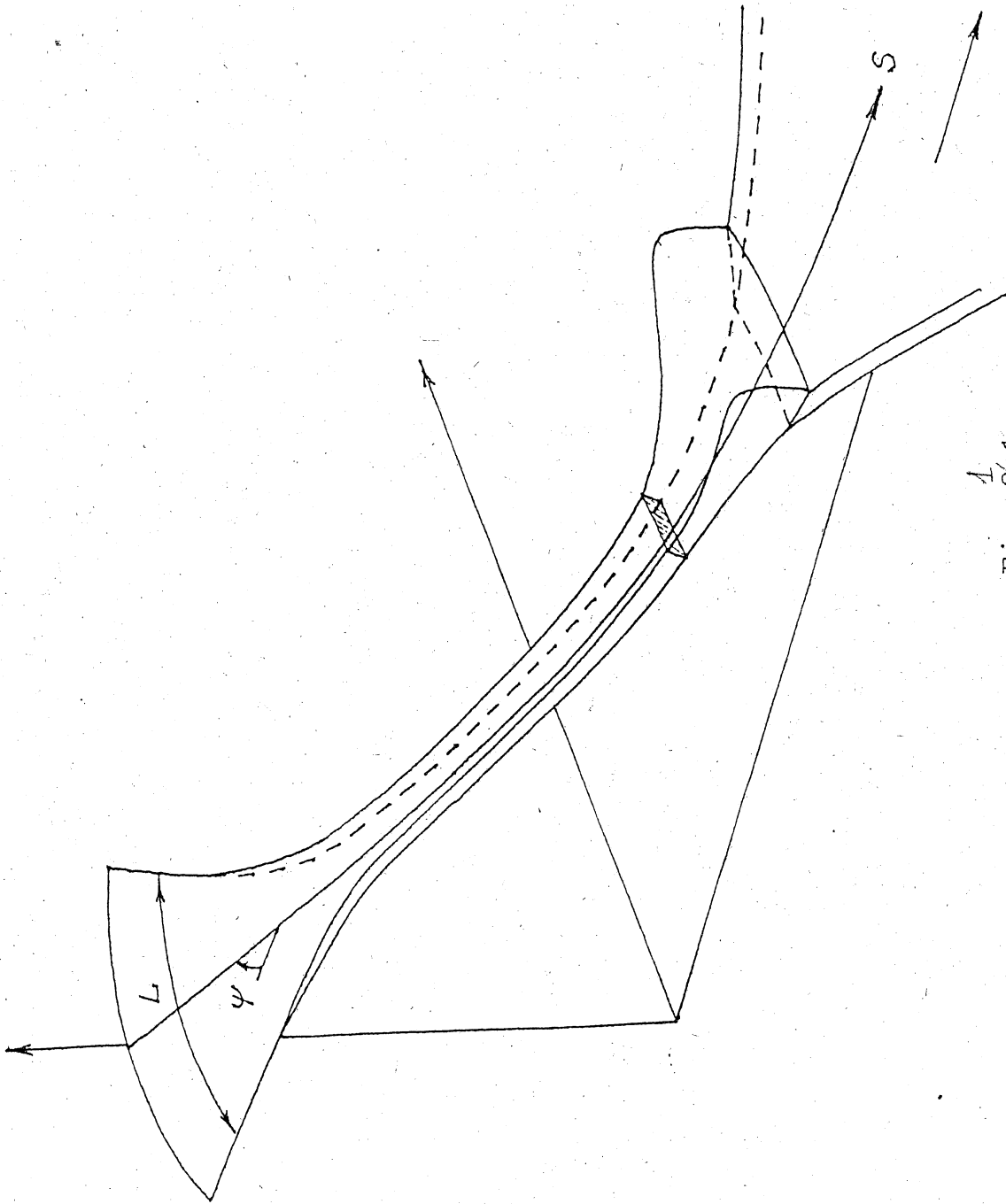
GRIGORIAN S.S., 1979: The new friction law and the mechanism of large scale rock falls and landslides. *Doklady Akademii Nauk SSSR*, v.244, N 4, (in Russian).

GRIGORIAN S.S., OSTROUMOV A.V., 1975: On mechanics of formation and collapse of rock masses deposits. *Scientific Reports of the Institute of Mechanics of the Moscow State University*, N 1724, (in Russian).

GRIGORIAN S.S., OSTROUMOV A.V., 1977: The mathematical model for slope processes of avalanche type. *Scientific Reports of the Institute of Mechanics of the Moscow State University*, N 1955, (in Russian).

GRIGORIAN S.S., OSTROUMOV A.V., STACHEIKO S.F., 1979: A simplified method for calculations of slope collapse processes. *Scientific Reports of the Institute of Mechanics of the Moscow State University*, N 2216, (in Russian).

Appendix
(the illustrations)



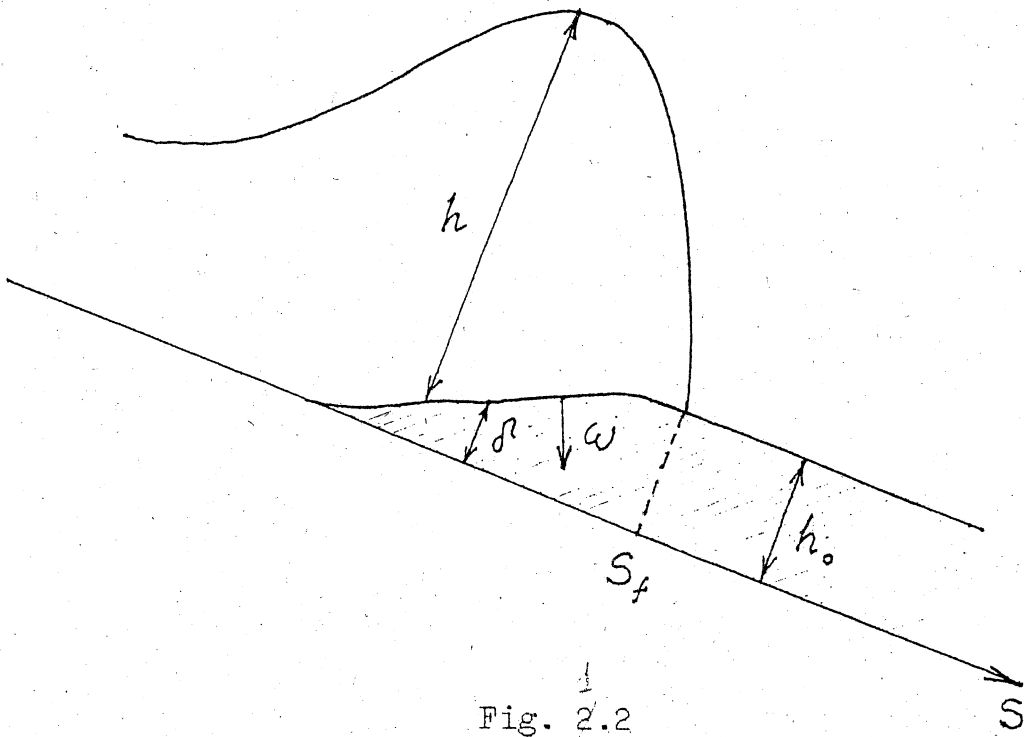


Fig. 2.2

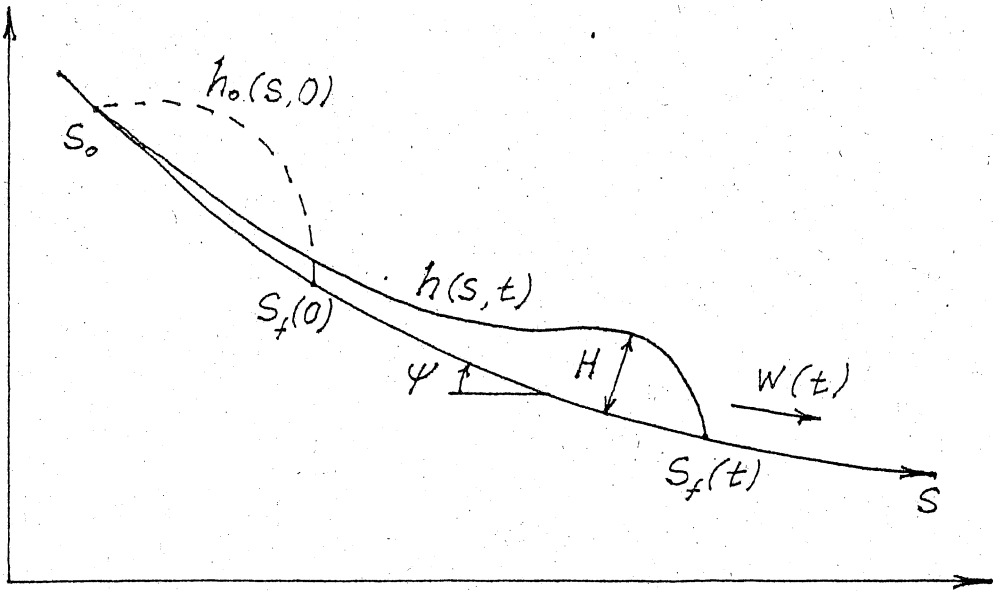


Fig. 2.3

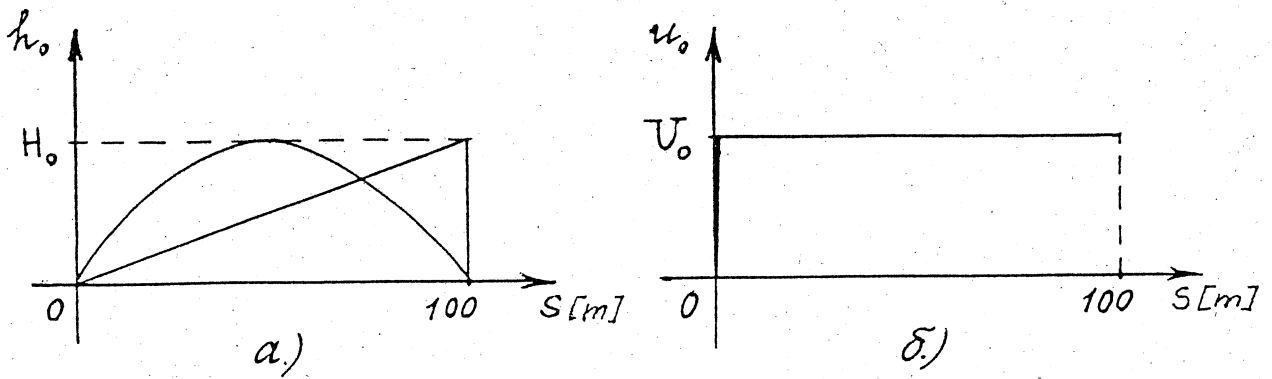
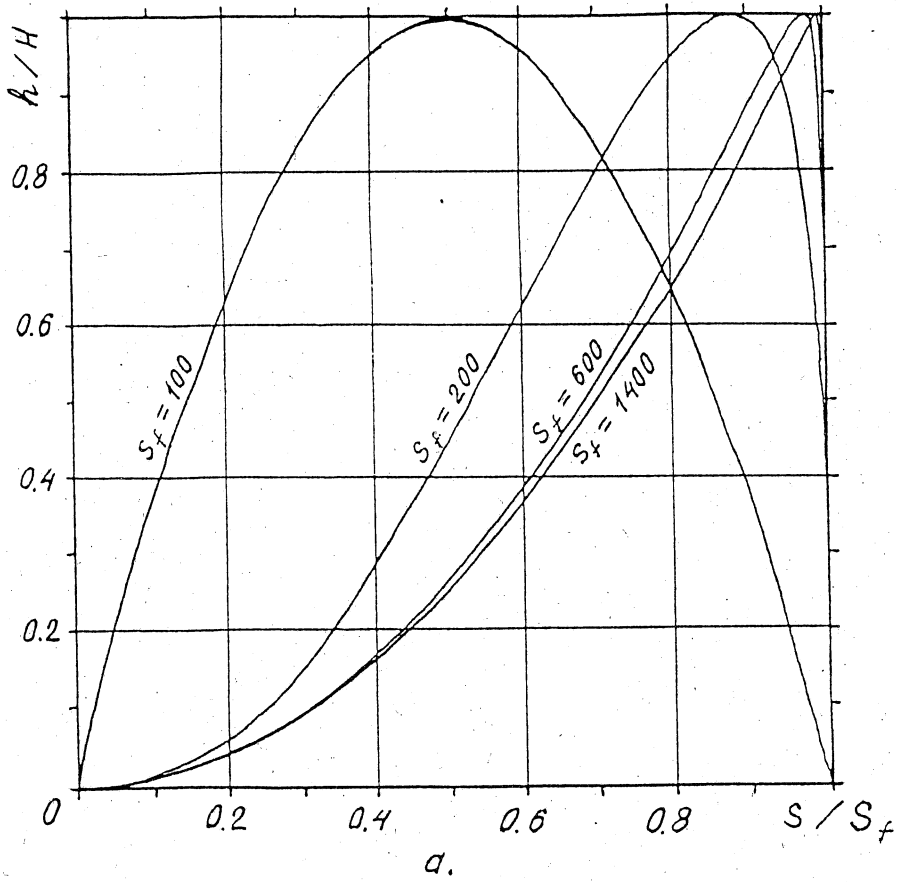
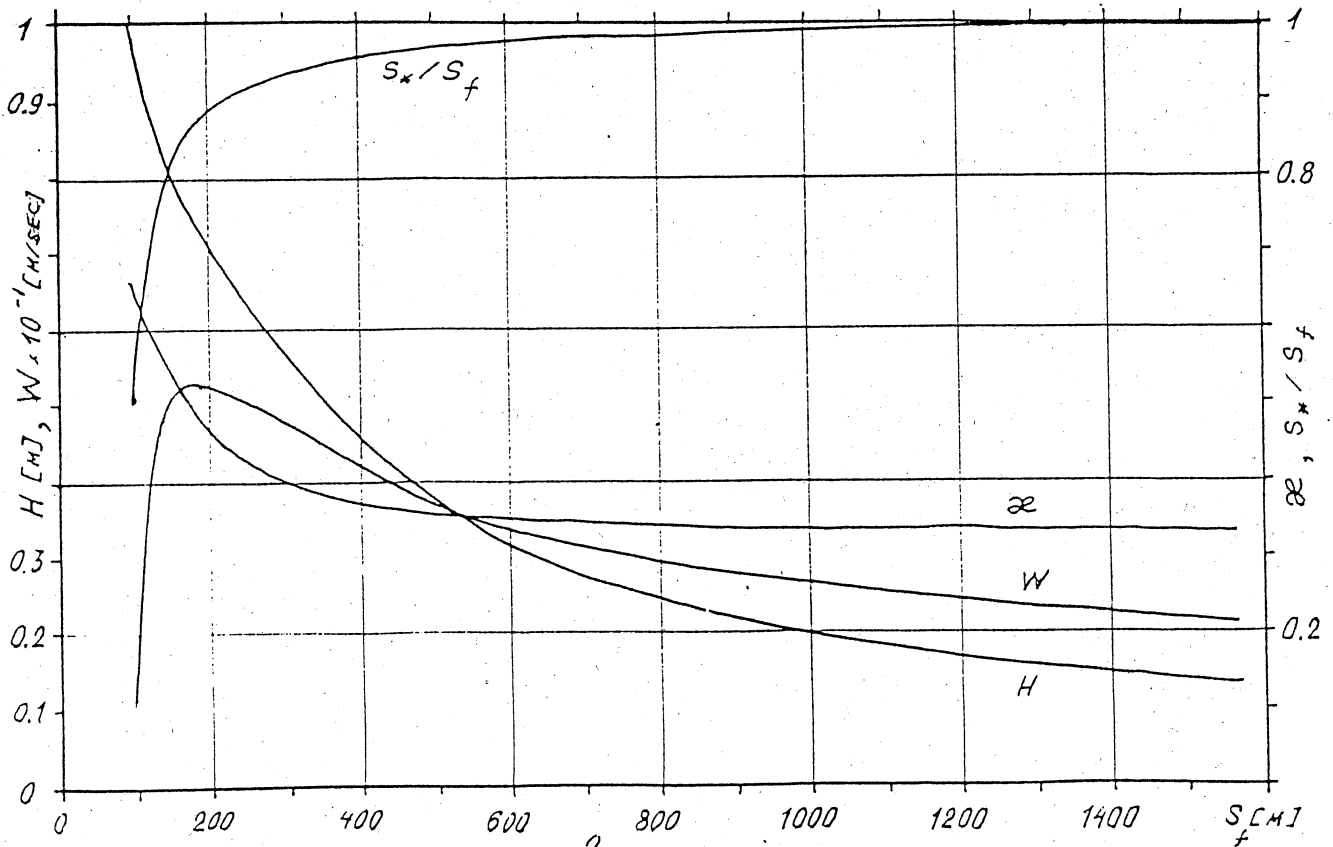


Fig. 4.1

Variant N 1



$M = 0.5$
 $K = 0.02$
 $\rho = 50 \frac{\text{kg} \cdot \text{s}^2}{\text{m}^4}$
 $\tau_* = 1000 \frac{\text{kg}}{\text{m}^2}$



B.
 3.
 Fig. 4.2

Variant N 2

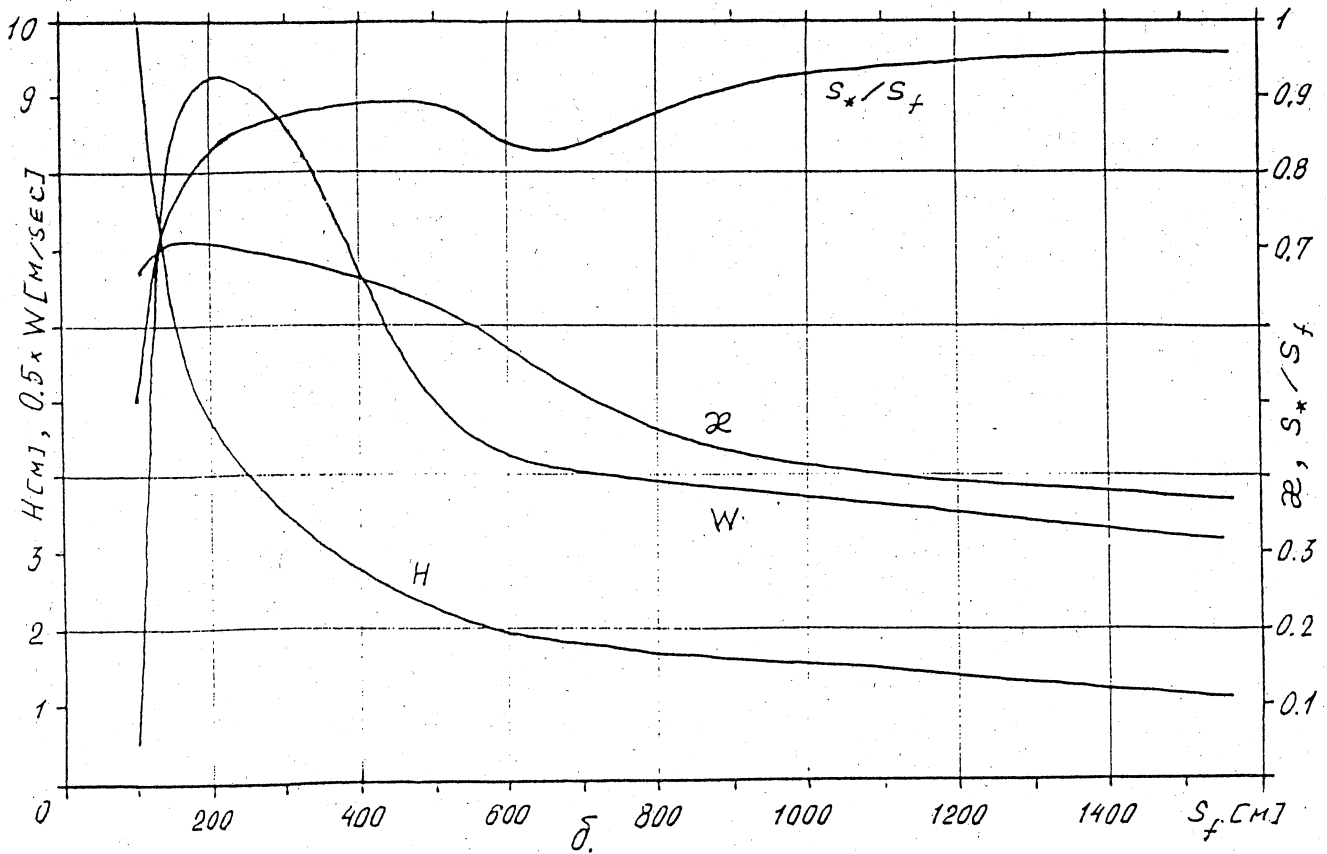
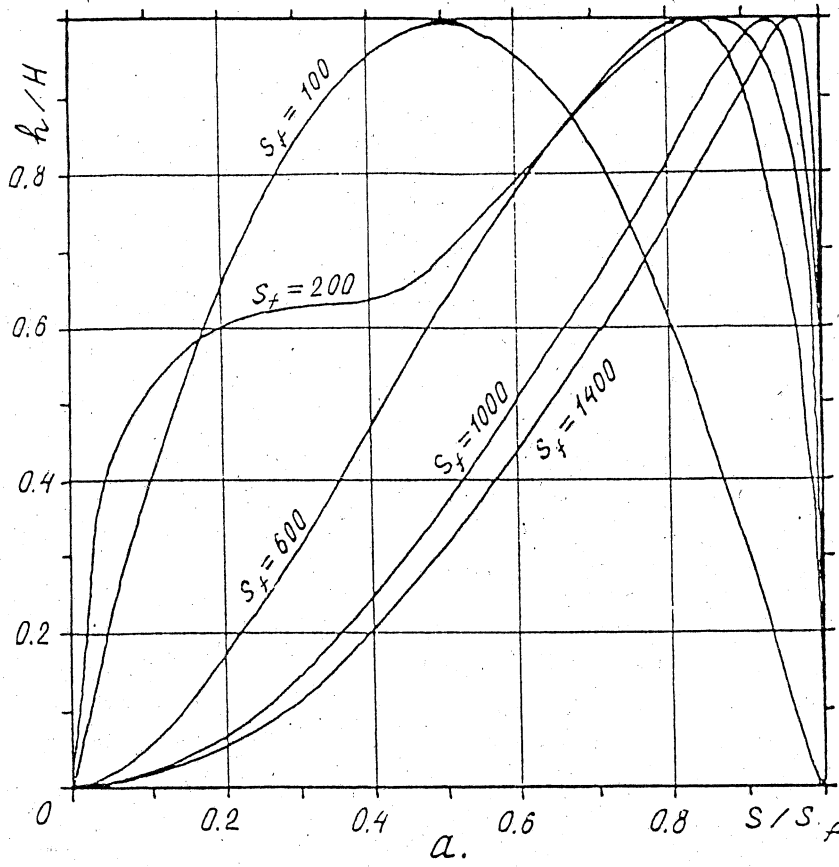


Fig. 34.3

Variant N 3

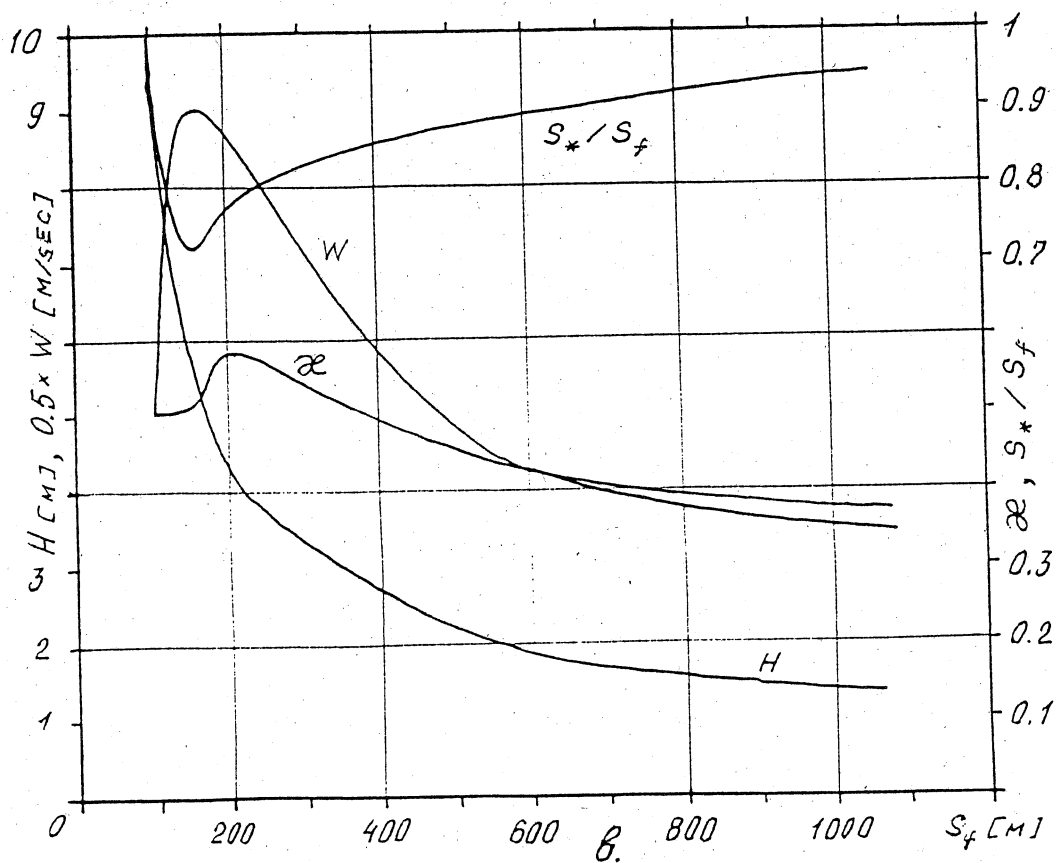
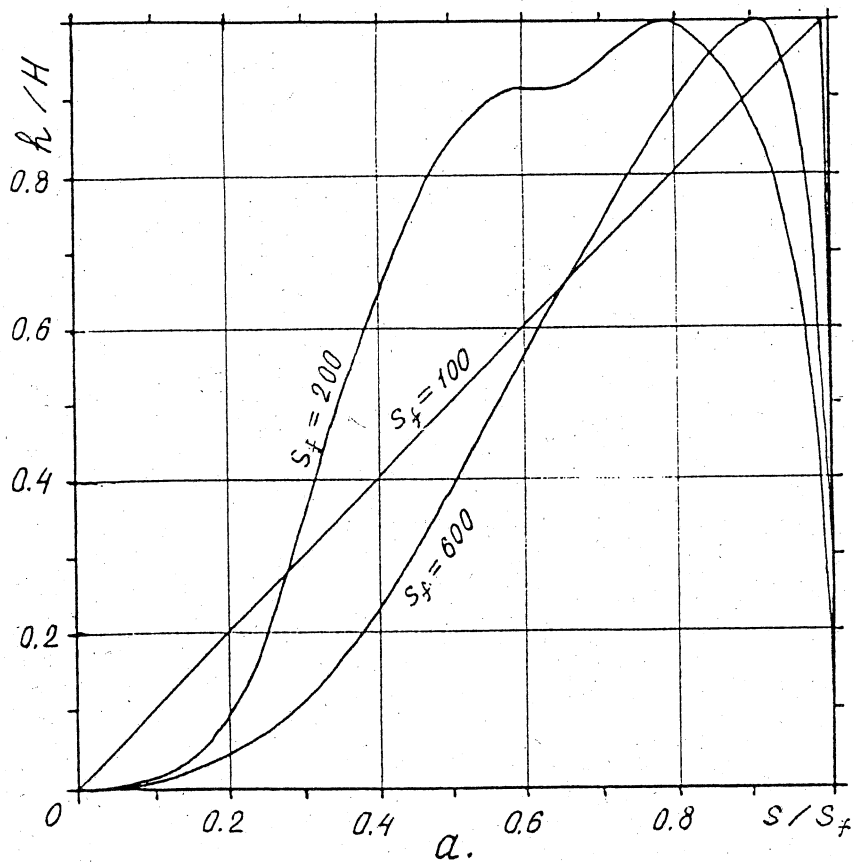
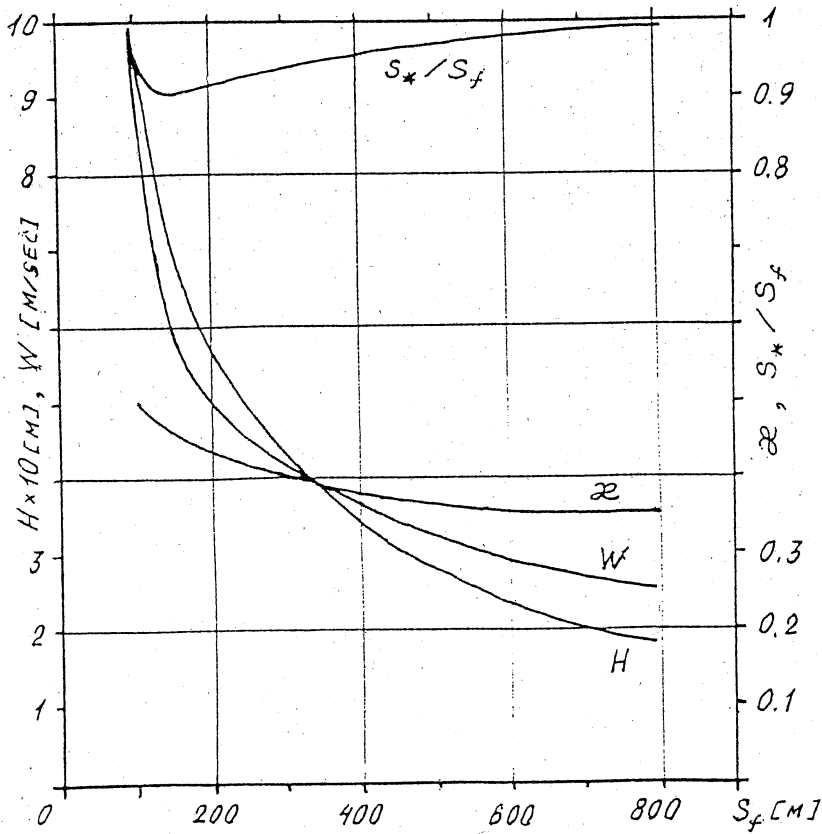
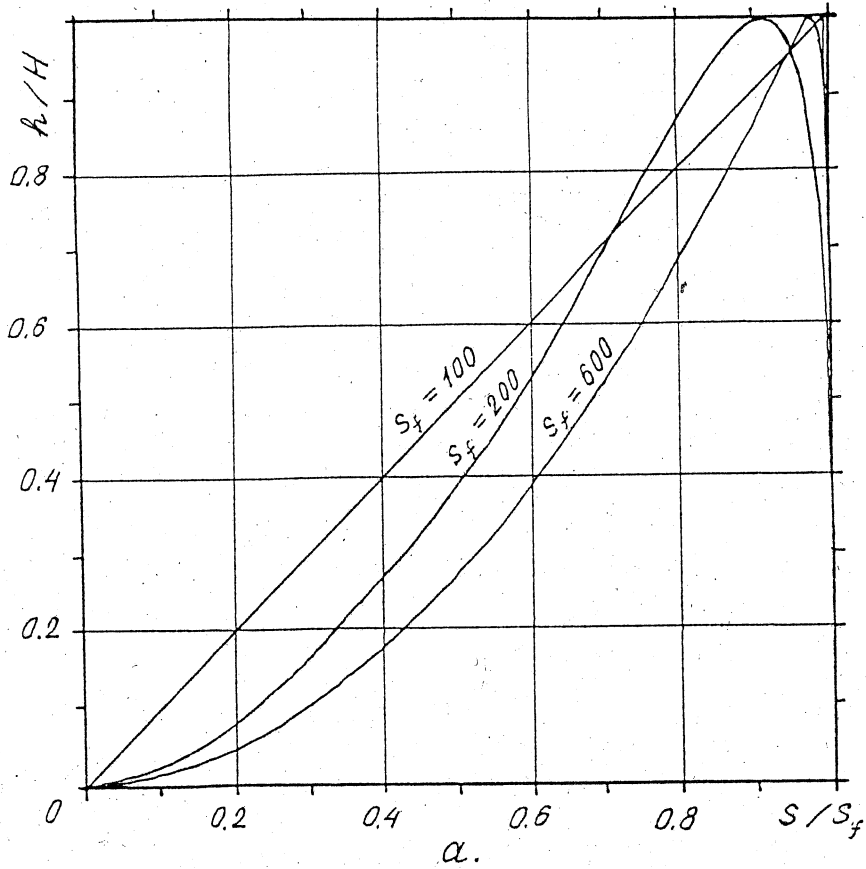


Fig. 4.4

Variant N 4.



B.
3
Fig. 4.5

Variant N 5

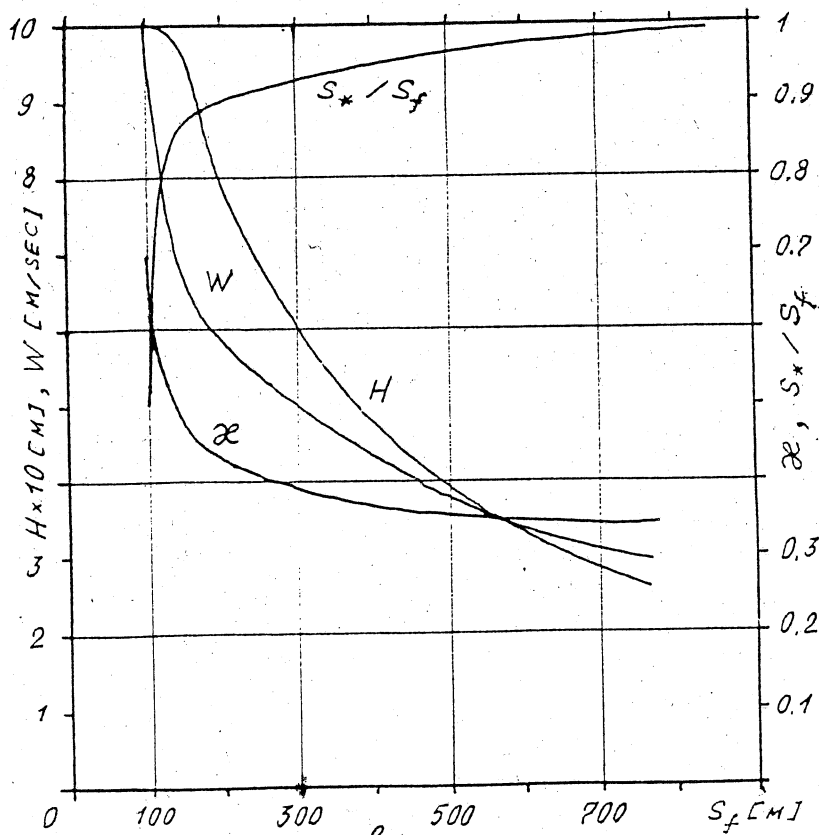
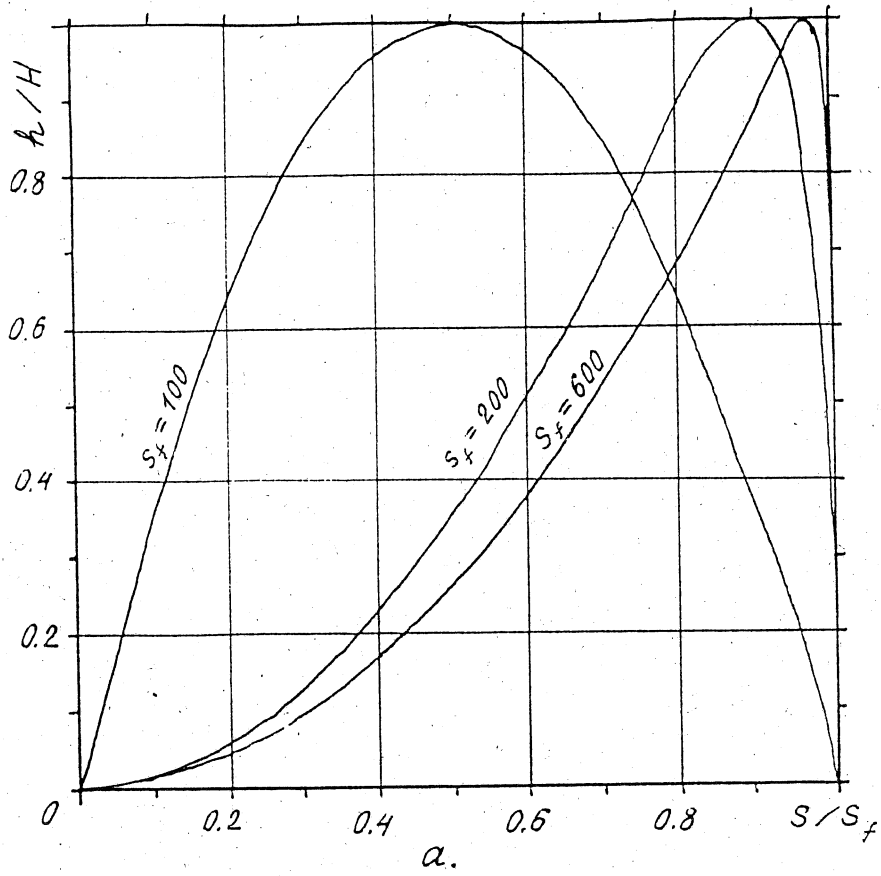
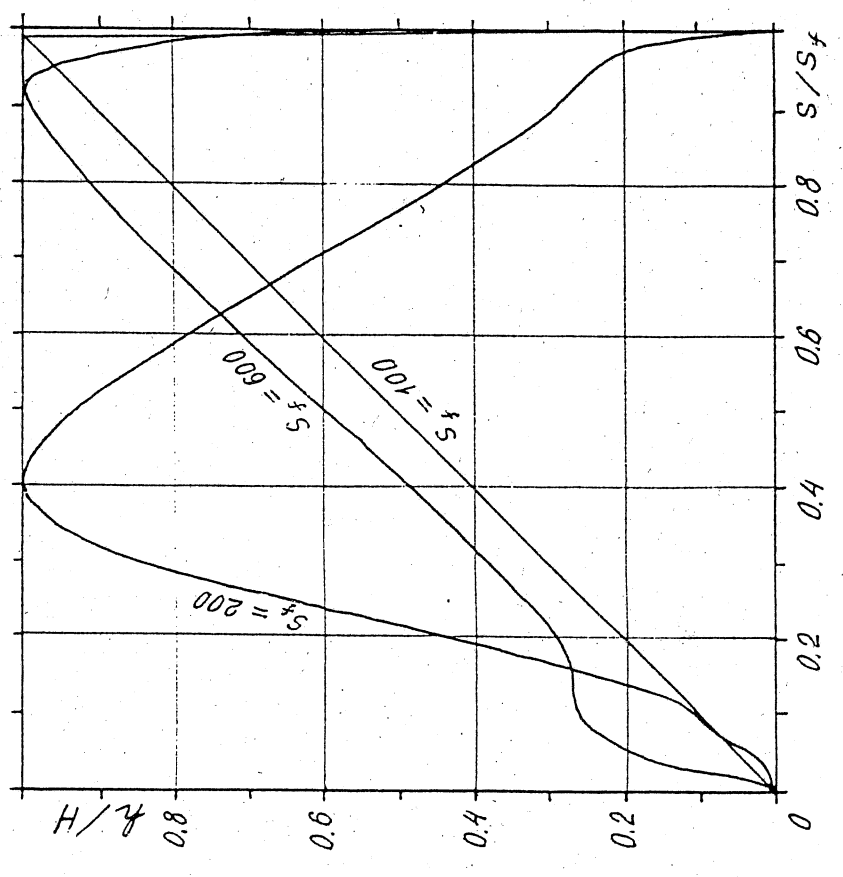
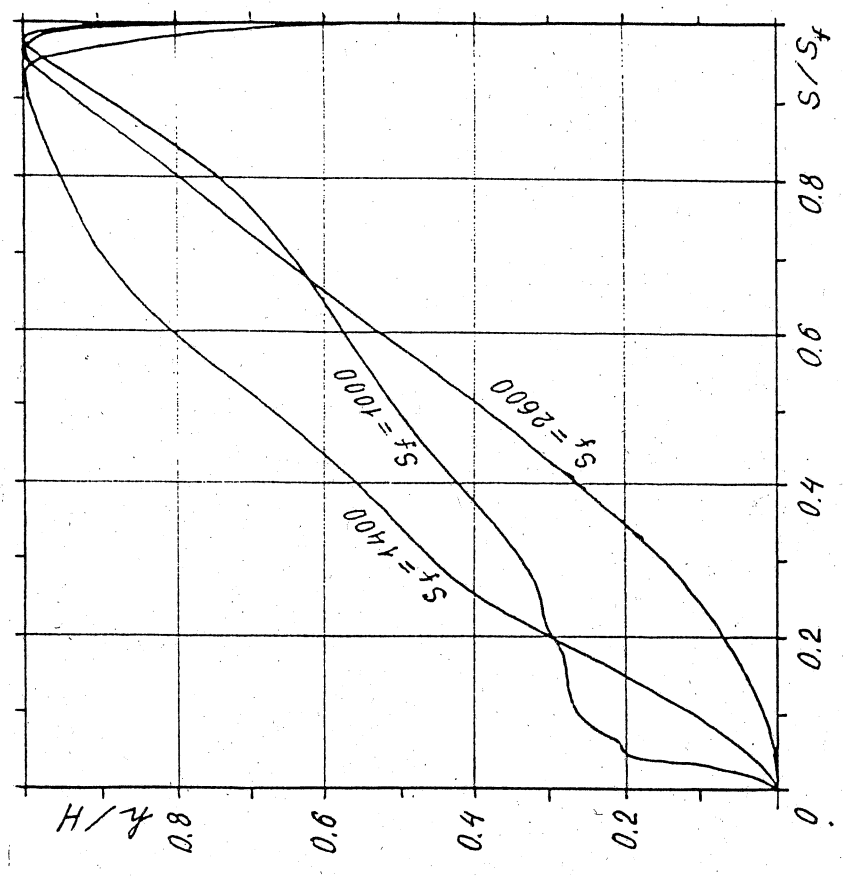


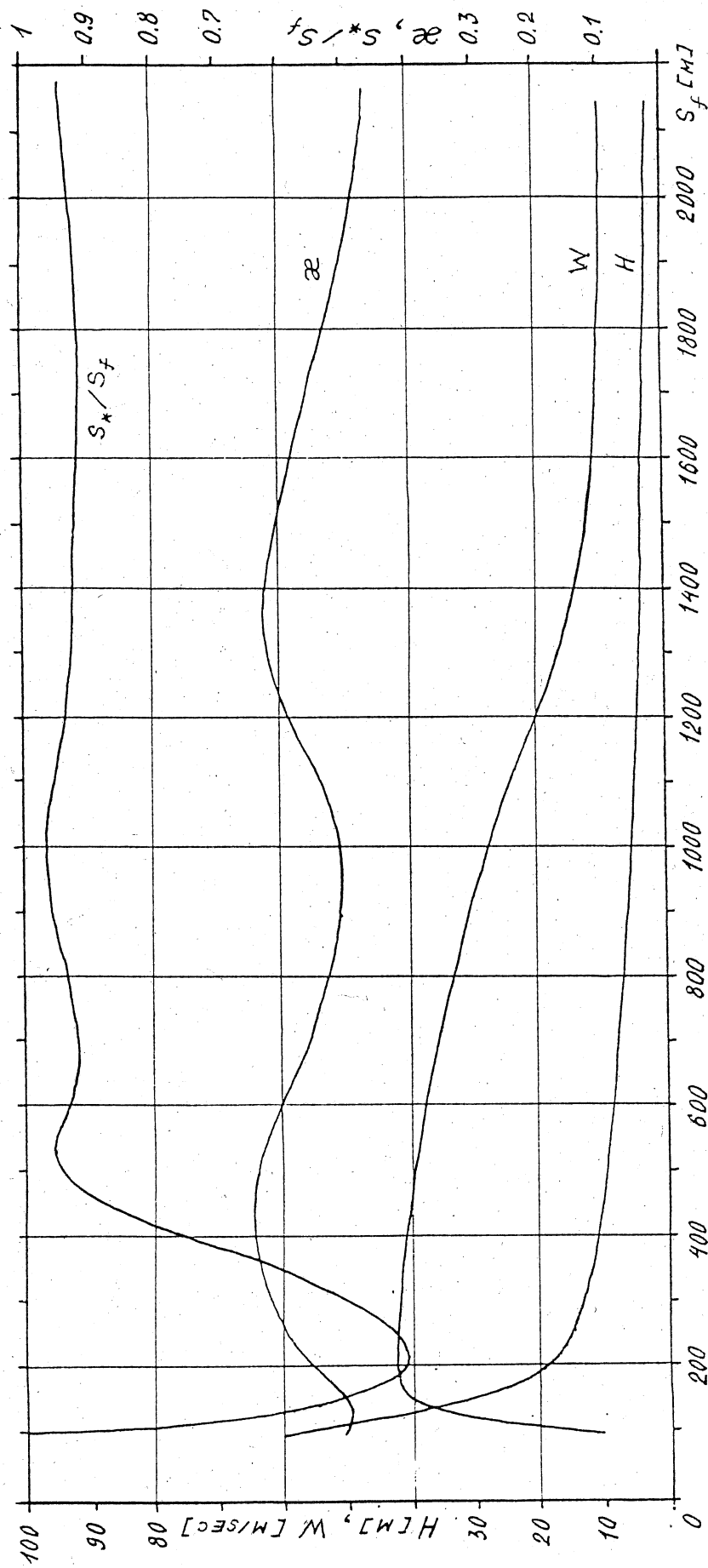
Fig. 4.6

Variant N 6



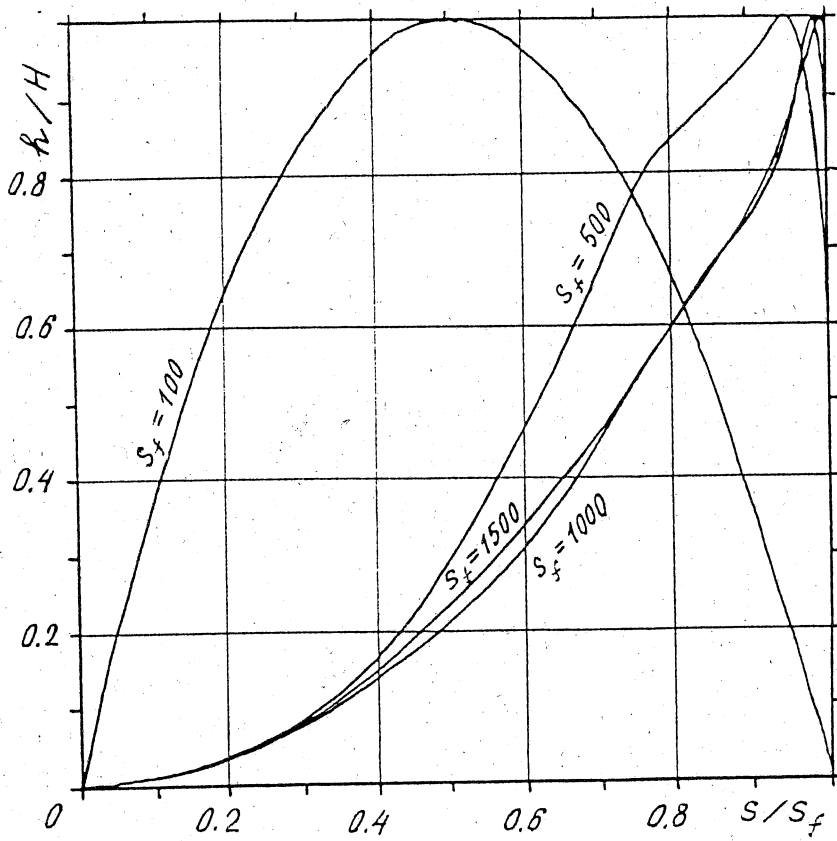
a.

Fig. A.7



6. 3
 FIG. A.7

Variant N 7



$\psi = 46^\circ$

a.

Fig. 3/4.8

Variant N 8

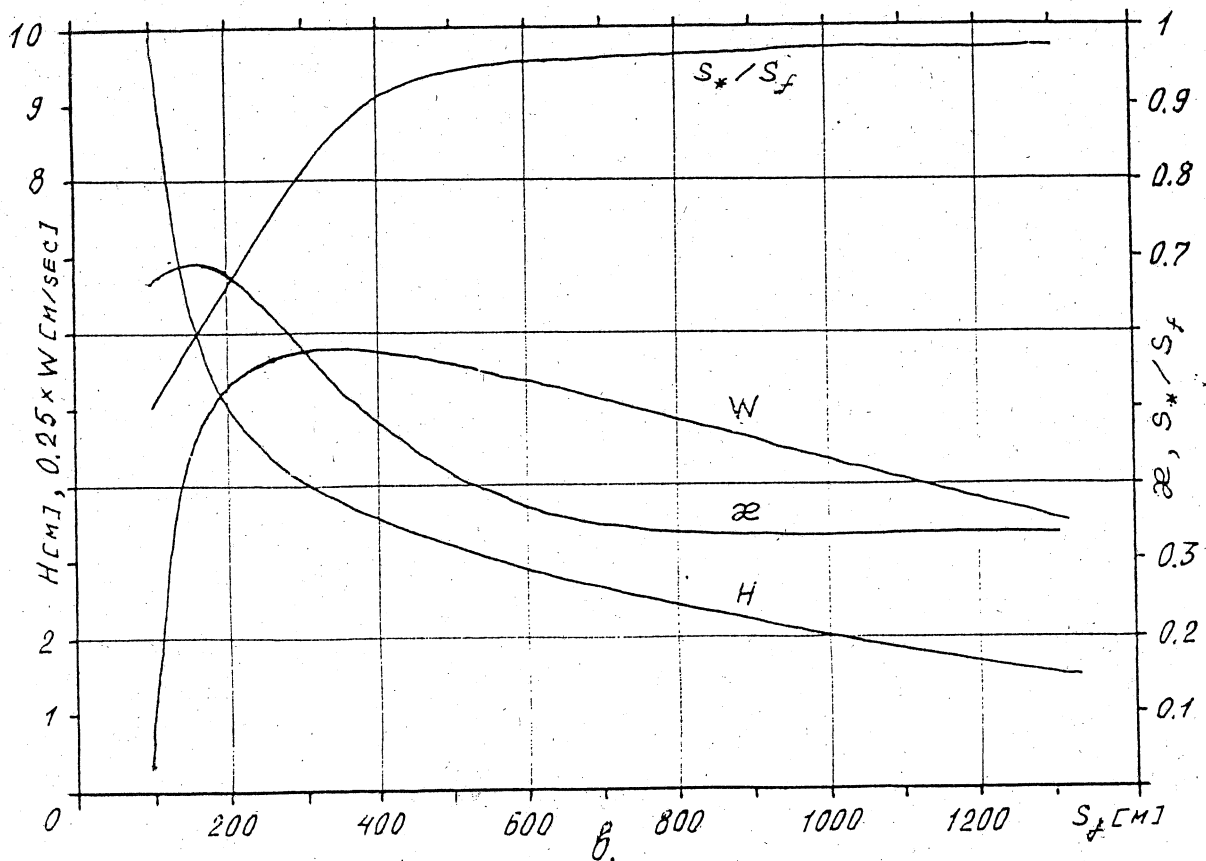
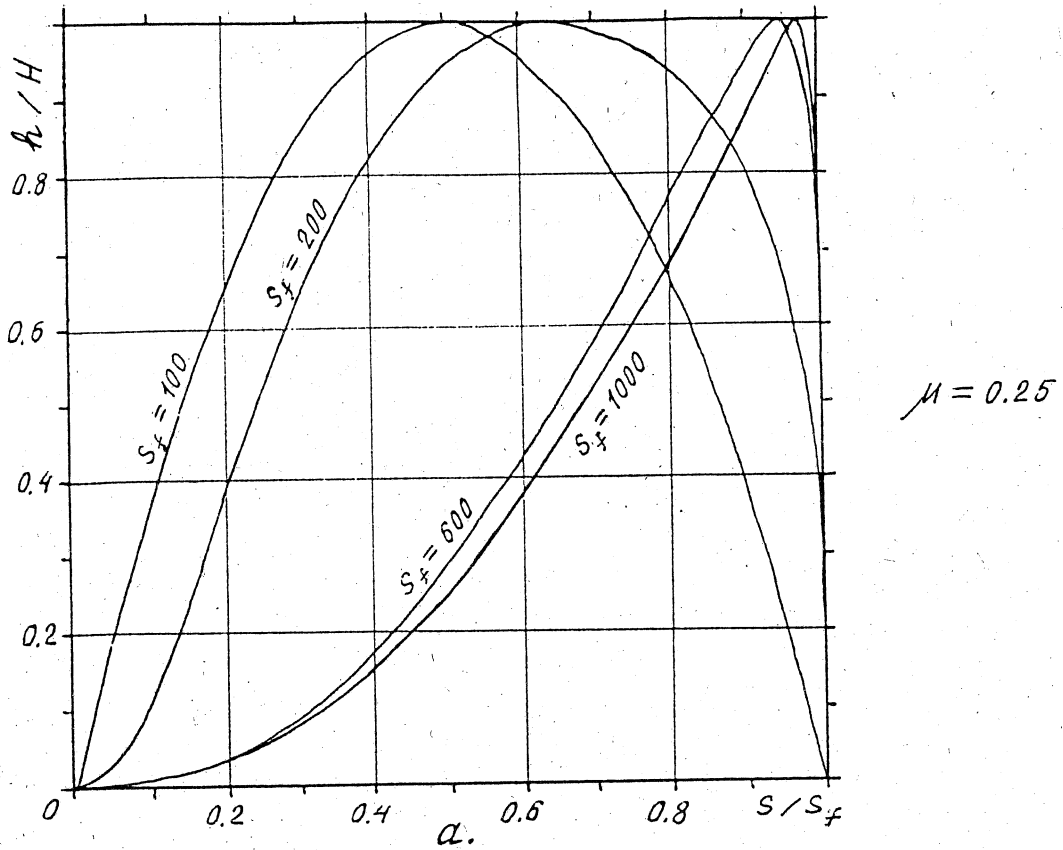


Fig. 3/4.9

Variant N 9

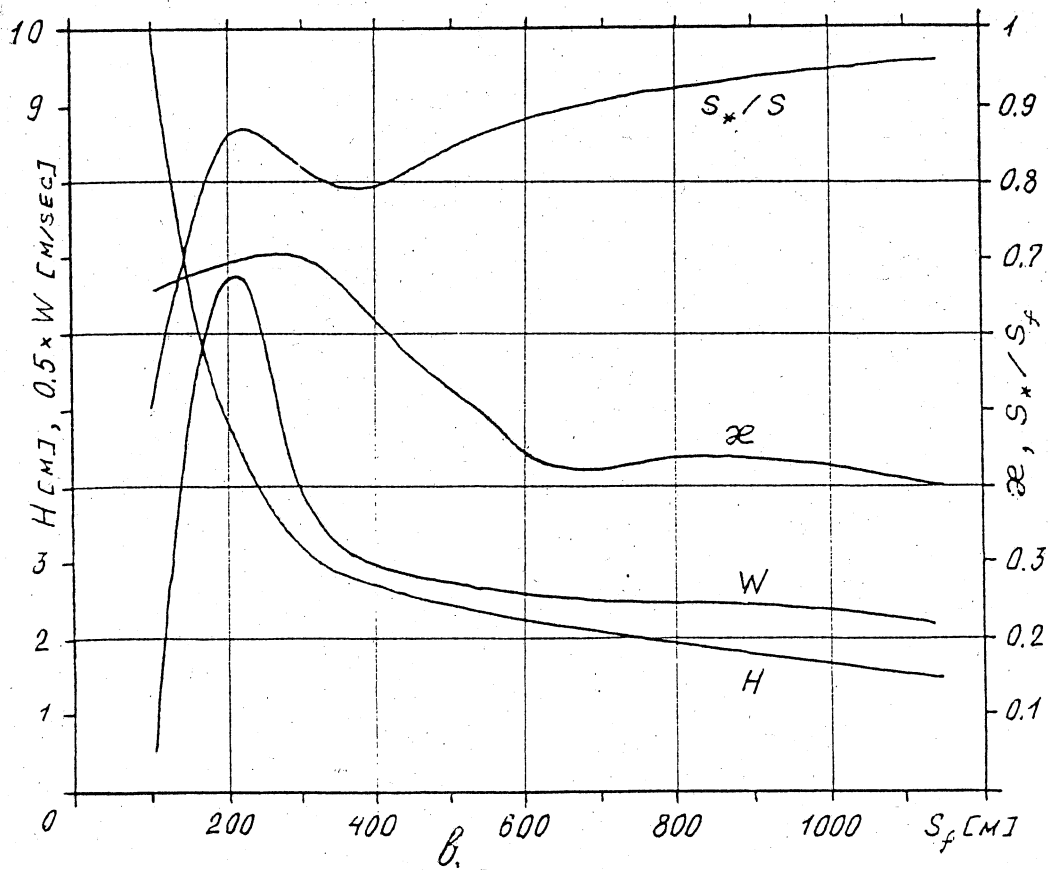
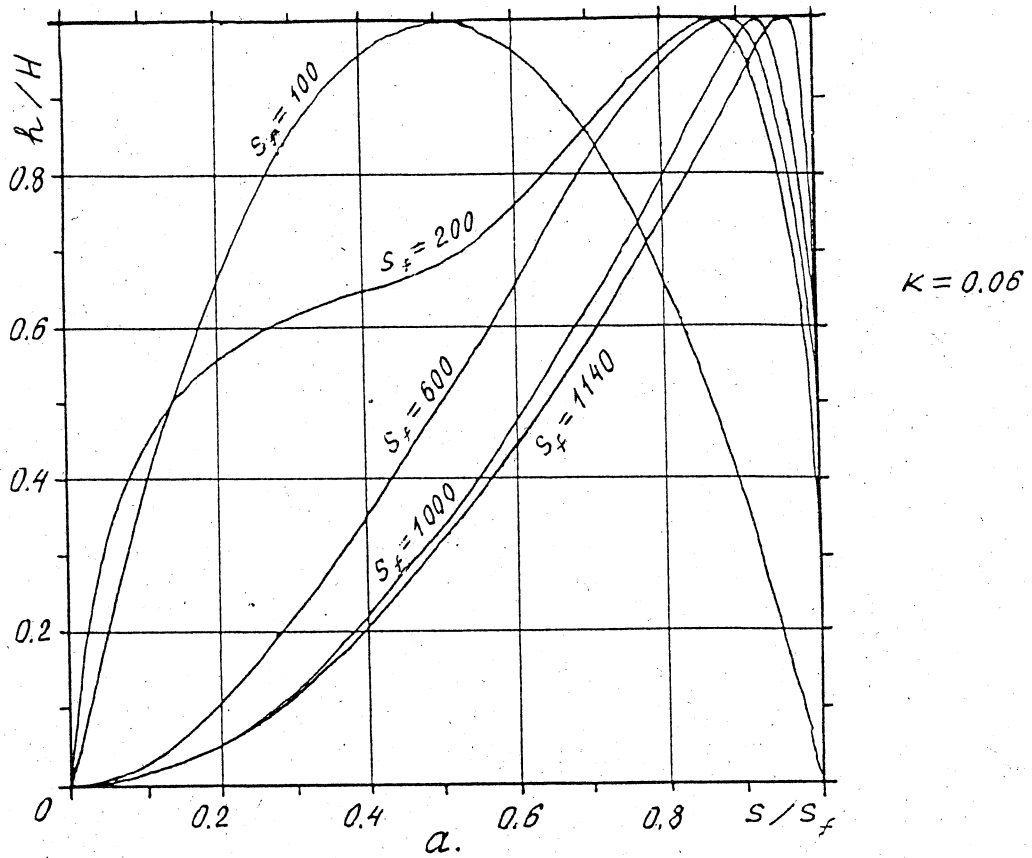


Fig. 3.4.10

Variant N 10

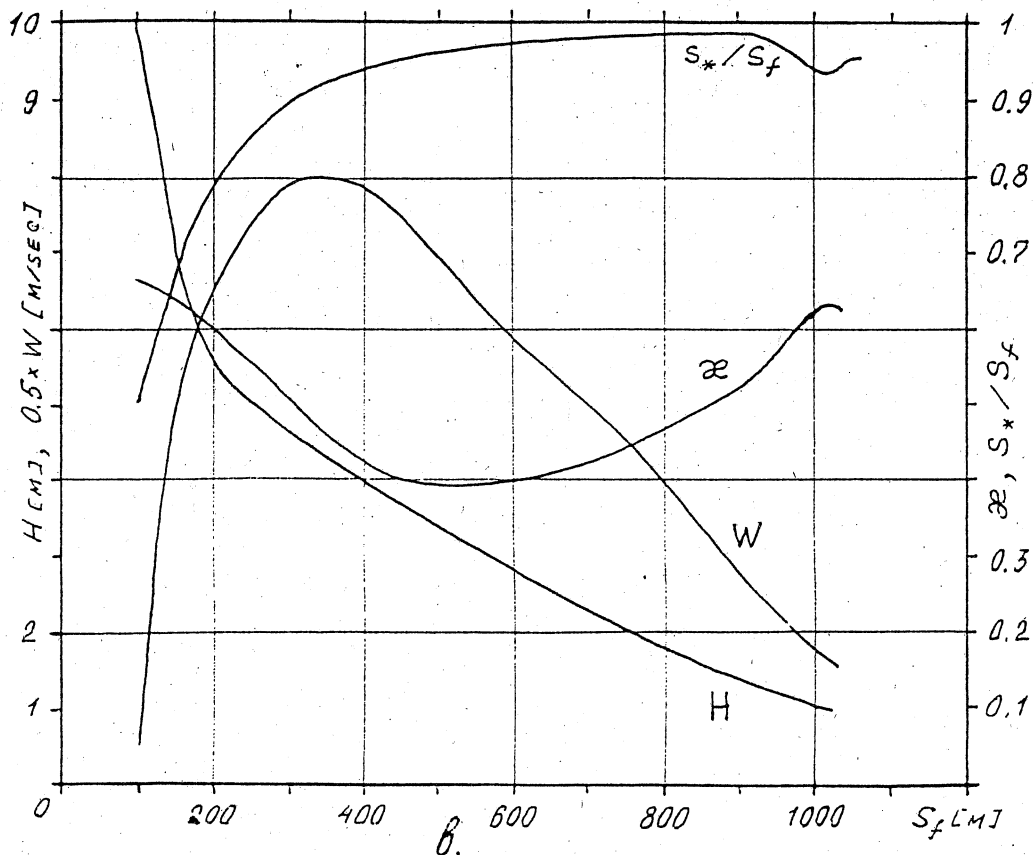
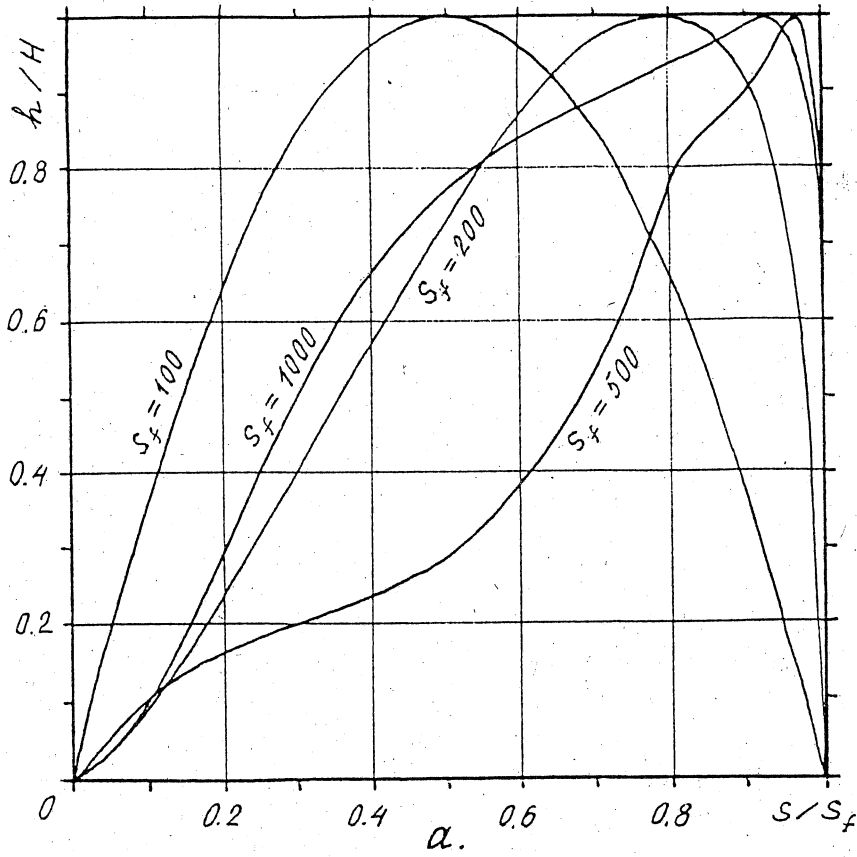


Fig. 4.11

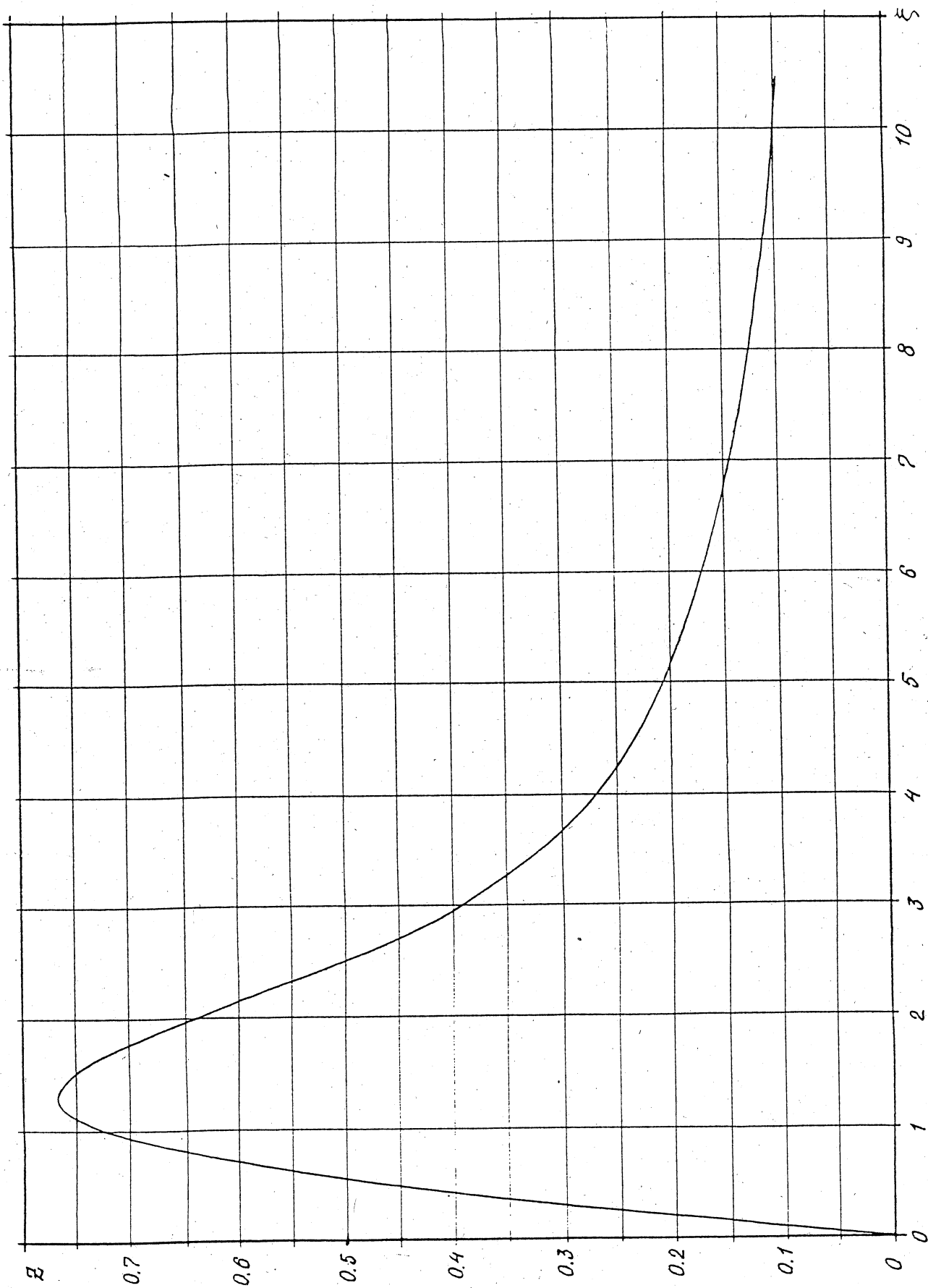


Fig. B.1 A

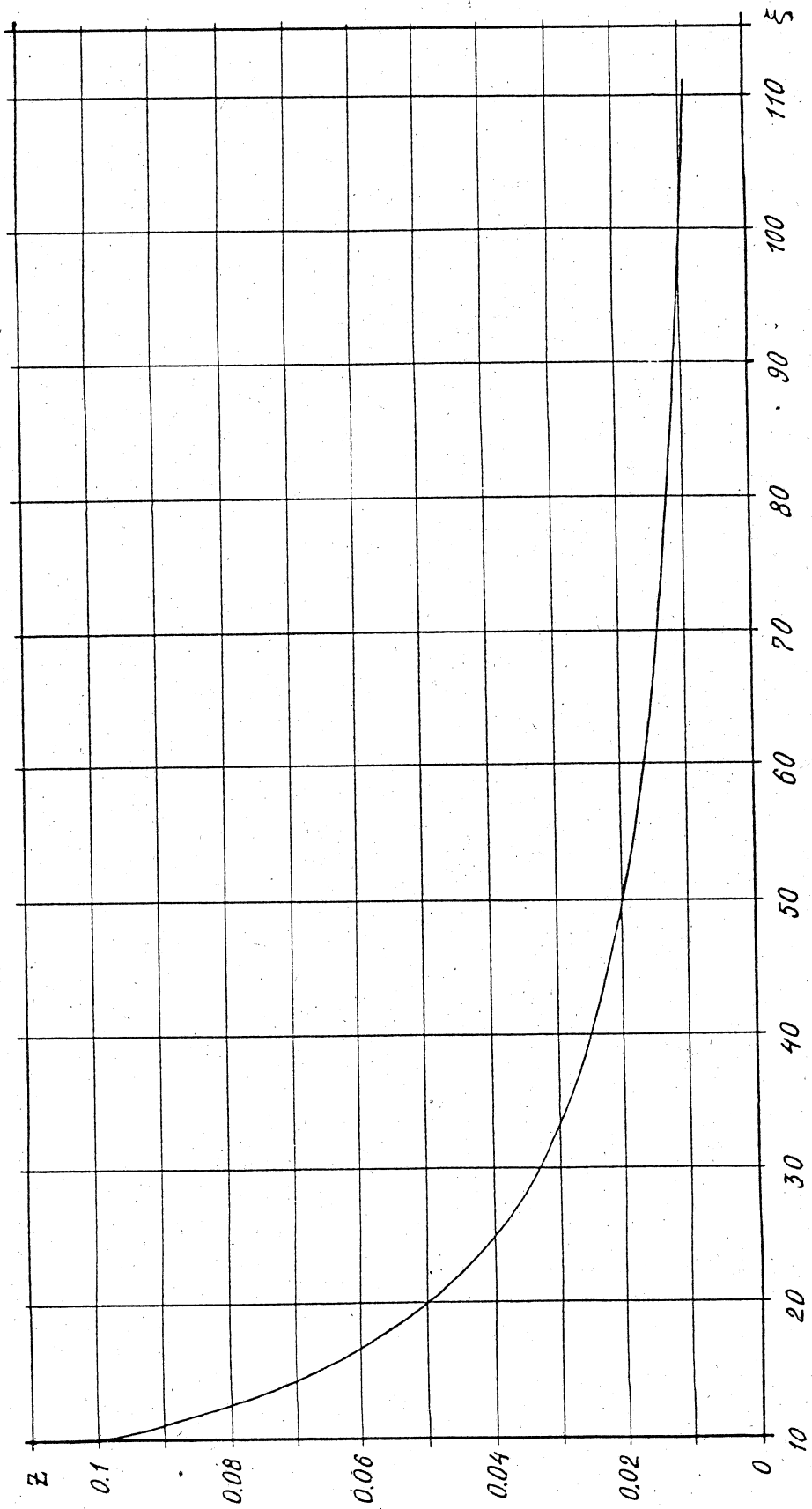


Fig. 5.1 B

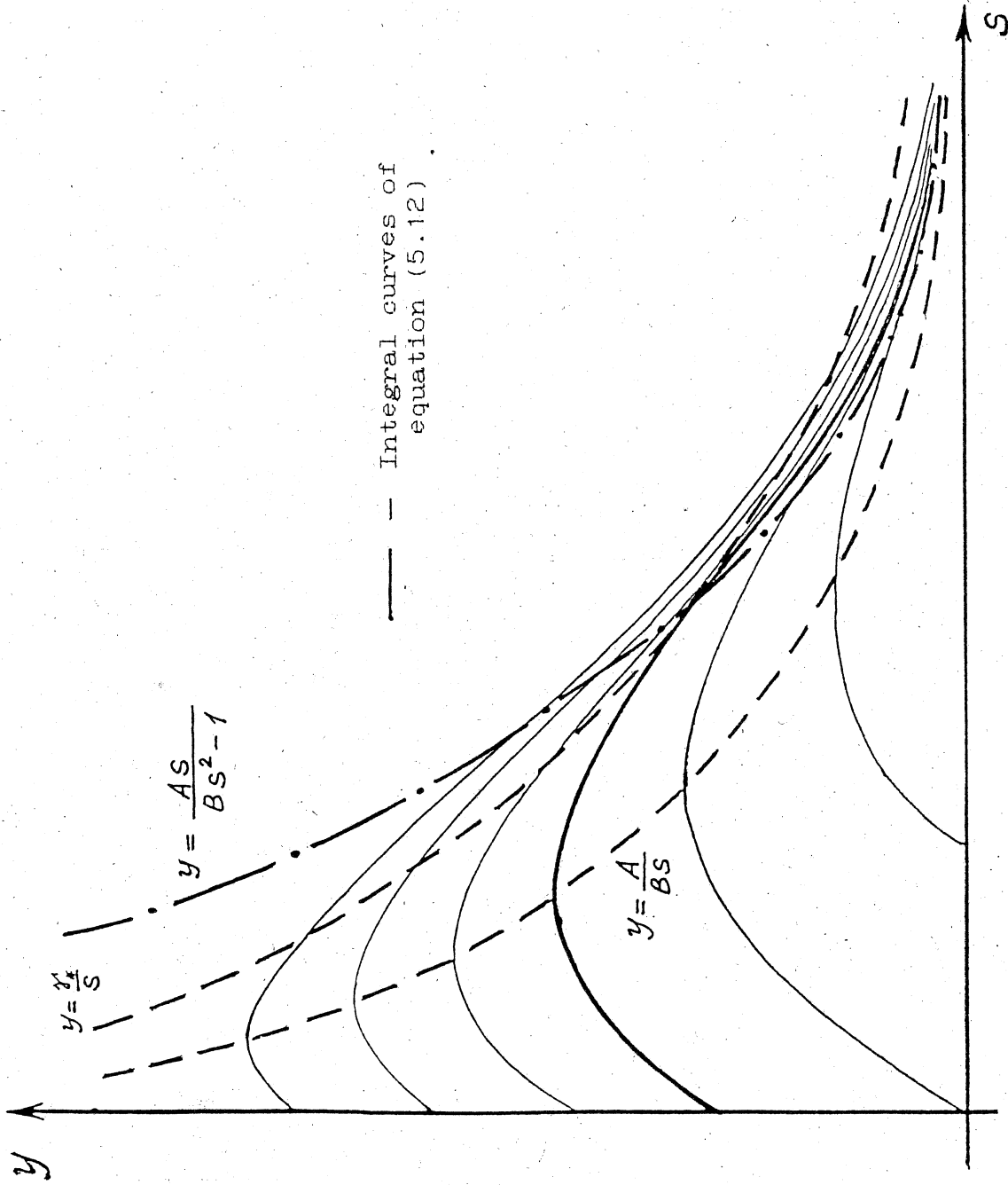


Fig. 5.2

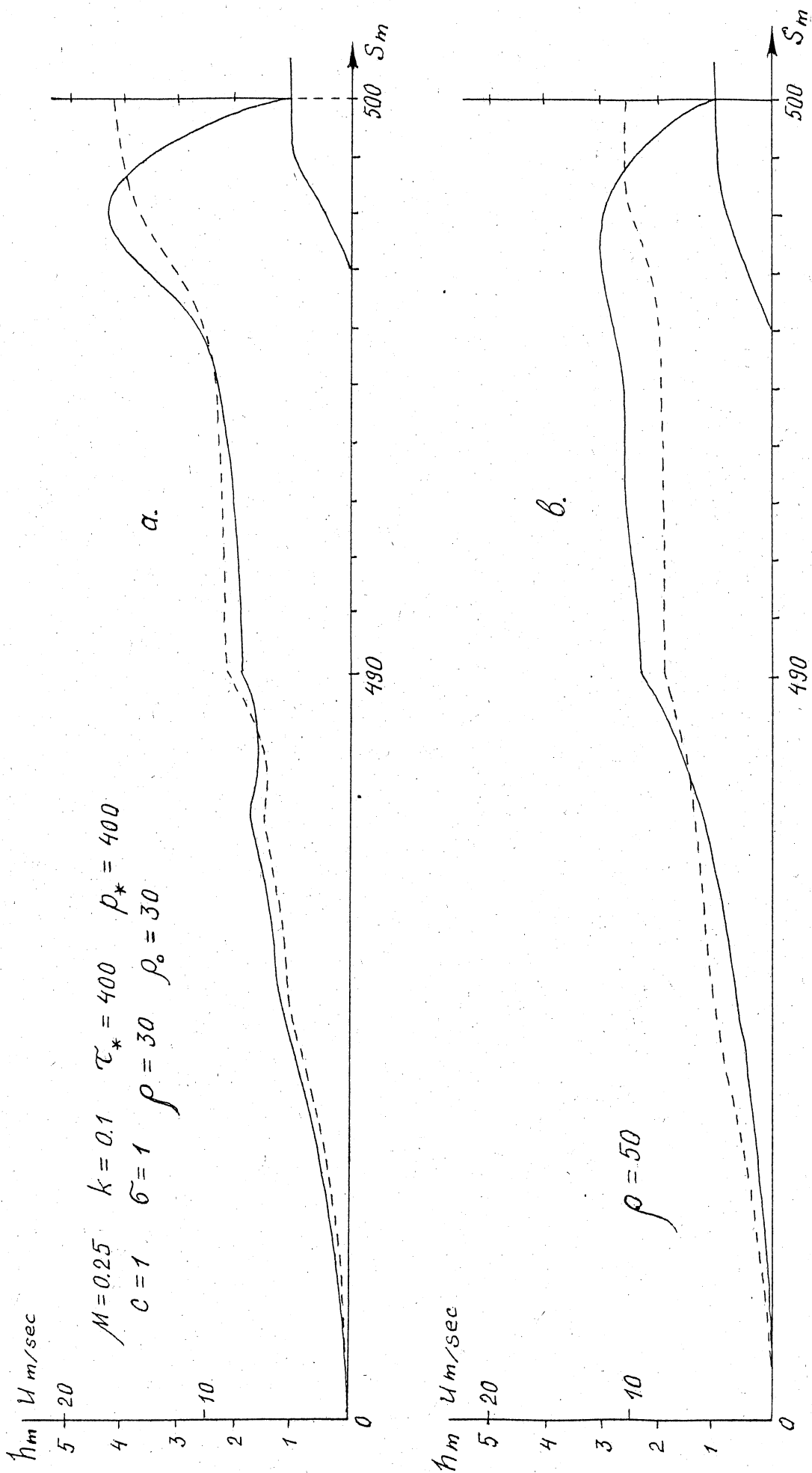
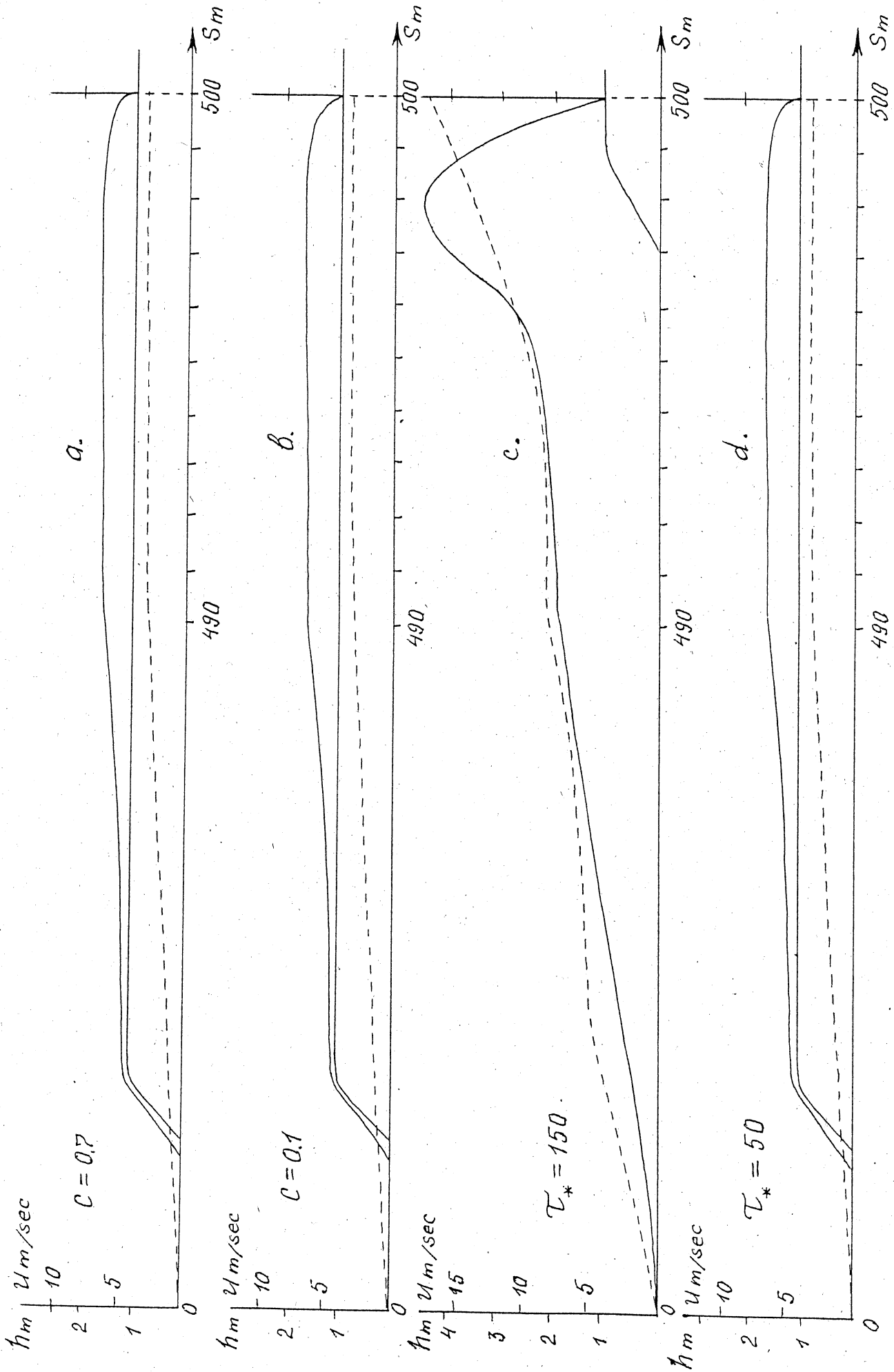
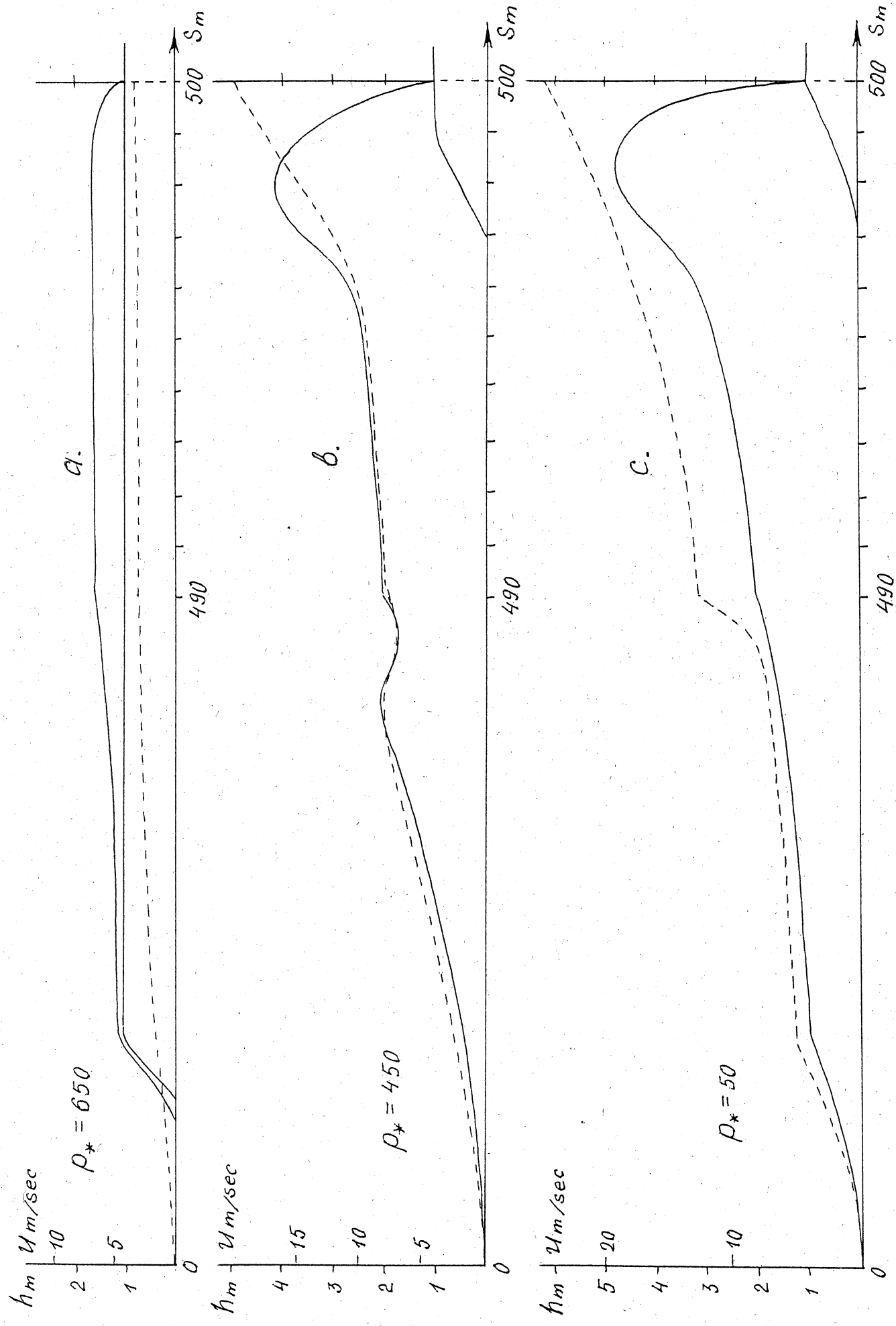


Fig. 7.1



6
Fig. 7.2



6
Fig. 7.3

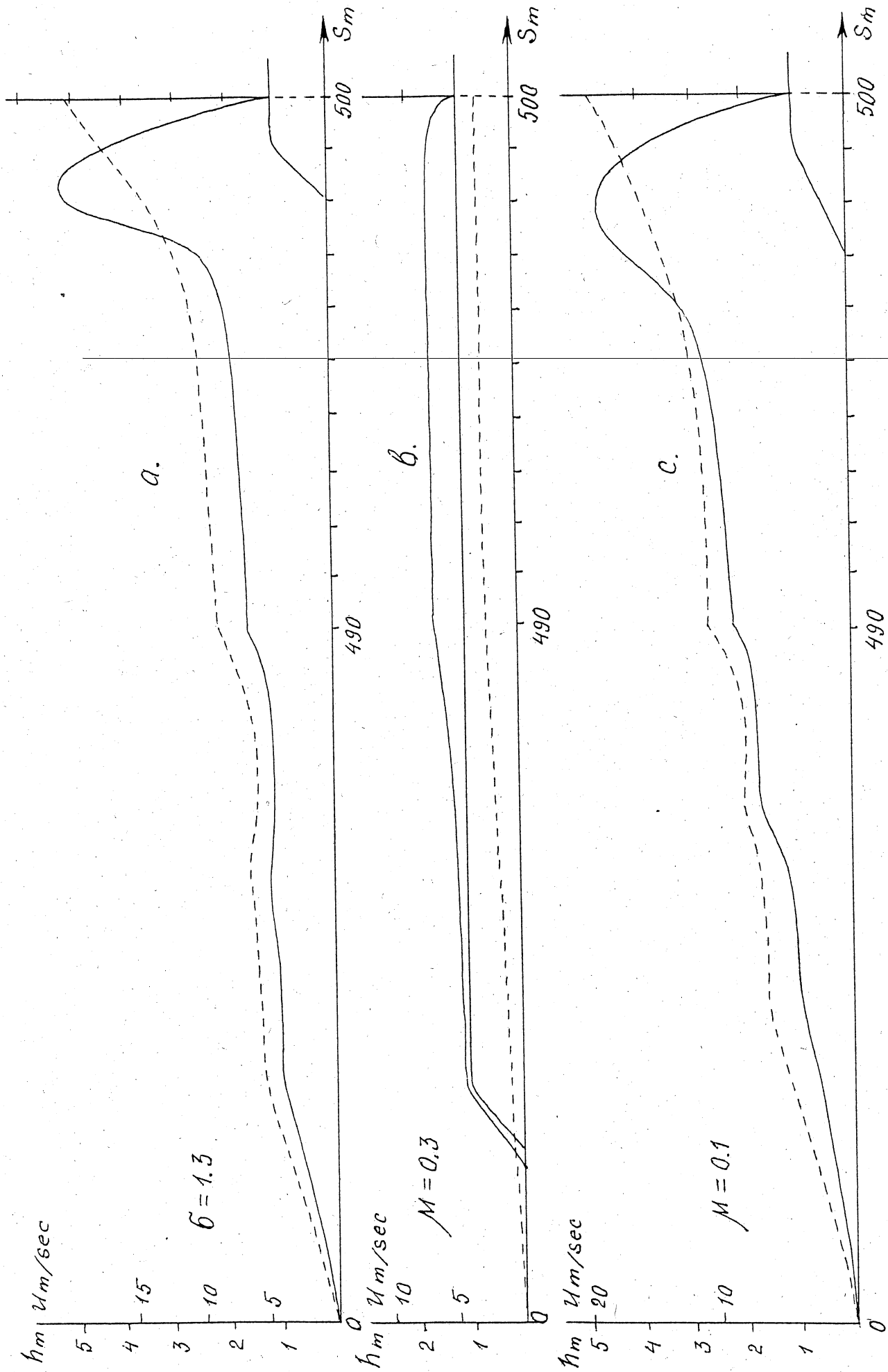
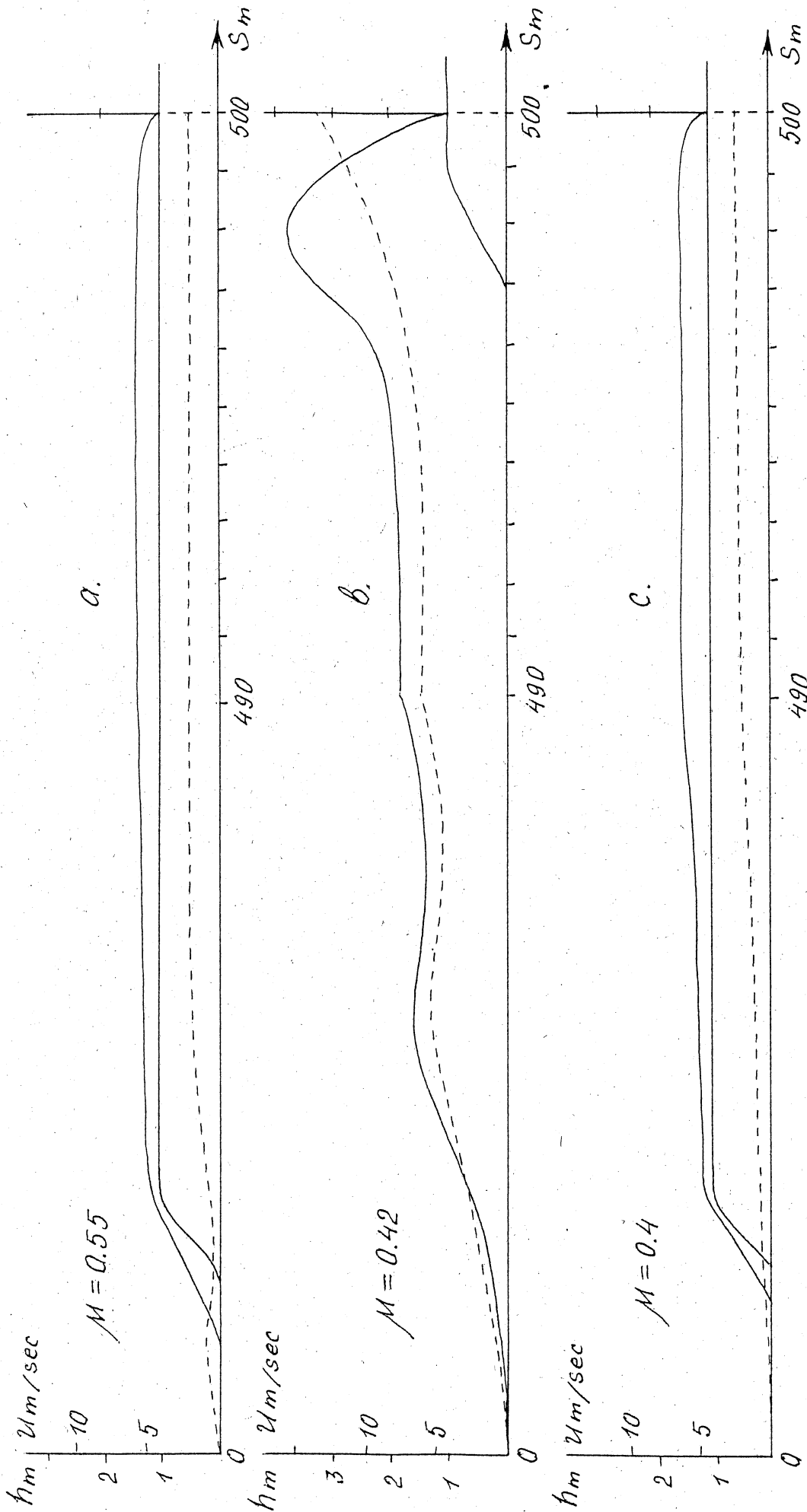


Fig. 7.4



6
Fig. 7.5

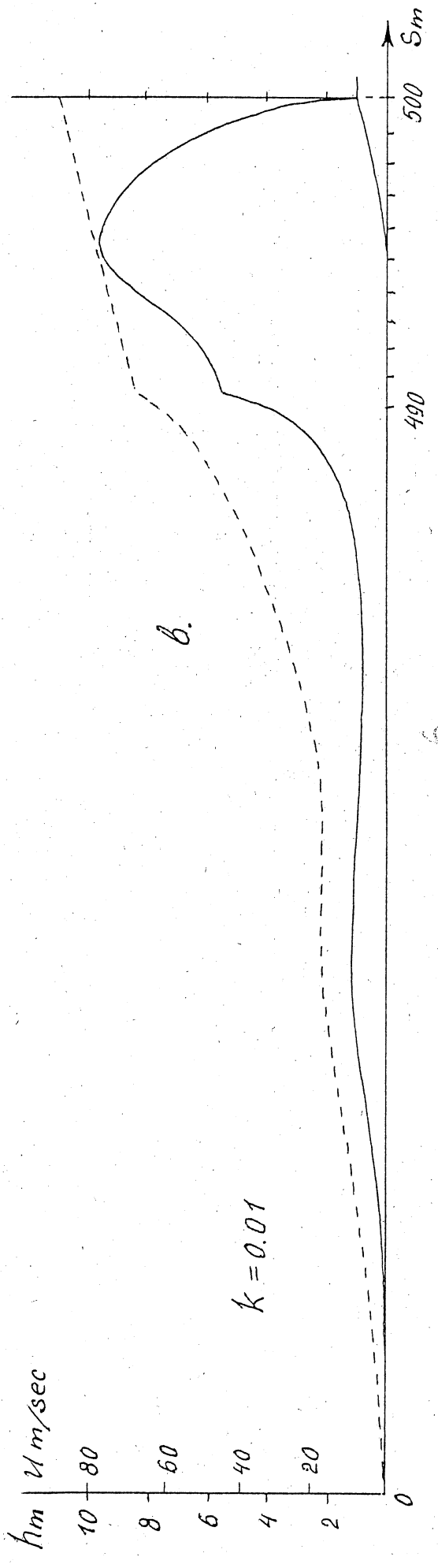
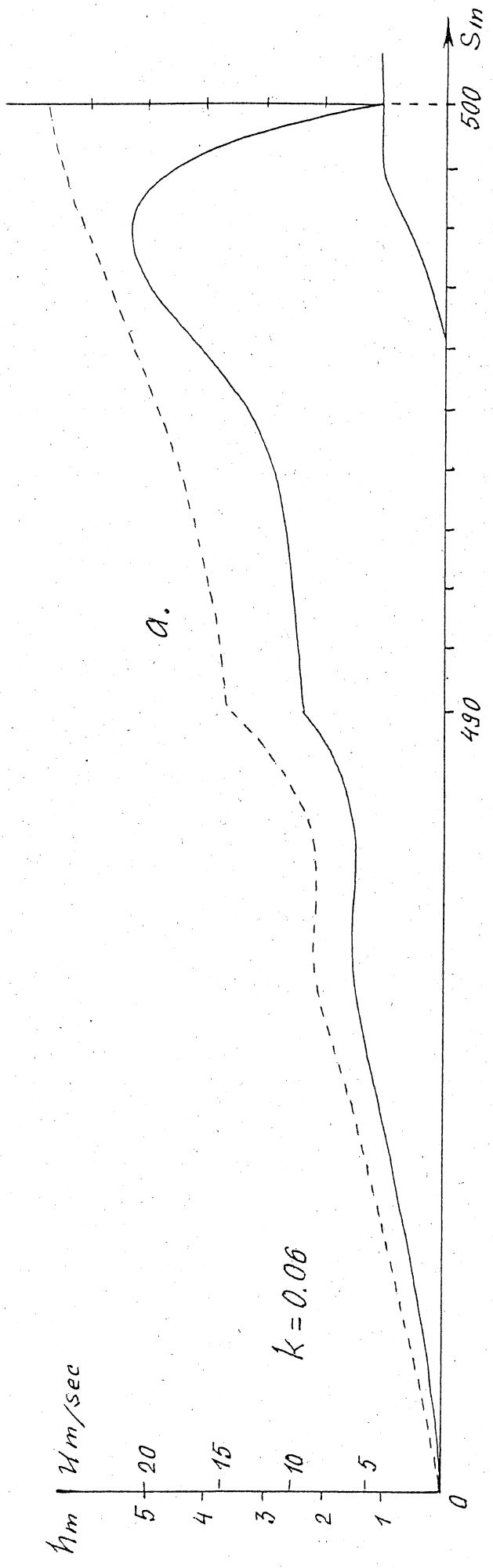
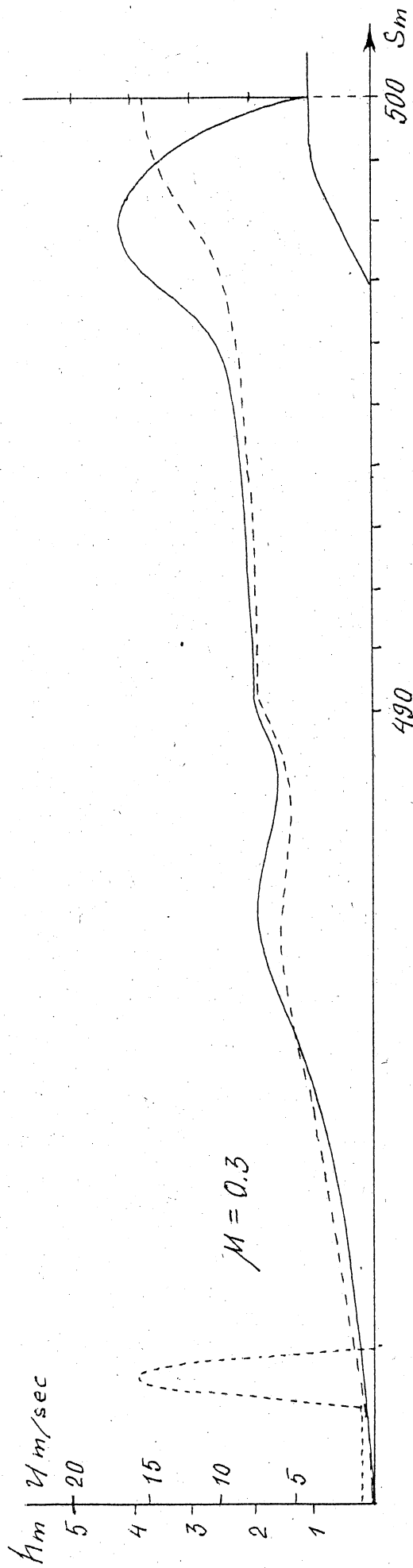


Fig. 7.6



6
FIG. 7.7